Modeling circulation and thermal structure in Lake Michigan: Annual cycle and interannual variability

Dmitry Beletsky

Department of Naval Architecture and Marine Engineering, University of Michigan, Ann Arbor, Michigan, USA

David J. Schwab

NOAA Great Lakes Environmental Research Laboratory, Ann Arbor, Michigan, USA

Abstract. A three-dimensional primitive equation numerical model was applied to Lake Michigan for the periods 1982–1983 and 1994–1995 to study seasonal and interannual variability of lake-wide circulation and thermal structure in the lake. The model was able to reproduce all of the basic features of the thermal structure in Lake Michigan: spring thermal bar, full stratification, deepening of the thermocline during the fall cooling, and finally, an overturn in the late fall. Large-scale circulation patterns tend to be cyclonic (counterclockwise), with cyclonic circulation within each subbasin. The largest currents and maximum cyclonic vorticity occur in the fall and winter when temperature gradients are low but wind stresses are strongest. The smallest currents and minimum cyclonic vorticity occur in spring and summer when temperature gradients are strong but wind stresses are weakest. All these facts are in agreement with observations. The main shortcoming of the model was that it tended to predict a more diffuse thermocline than was indicated by observations and explained only up to half of the variance observed in horizontal currents at timescales shorter than a day.

1. Introduction

The issue of potential climate change effects on Great Lakes hydrodynamics [*Lam and Schertzer*, 1999] raises the question of how to determine the background state of the lake's thermal structure and circulation. Currently, the only parameters with a sufficient amount of observations to allow for climatological averaging are surface temperature [*Schertzer and Croley*, 1999] and subsurface temperature measured at a few water intakes [*McCormick and Fahnenstiel*, 1999]. Subsurface water temperature and especially current data present the most significant challenge for describing the background state [*Beletsky et al.*, 1999b]. Hydrodynamic modeling data can certainly serve as a surrogate, but the accuracy of long-term numerical simulations of lake circulation has not been sufficiently tested. There has been significant progress in hydrodynamic modeling of short-term hydrodynamic processes in the Great Lakes [*Schwab*, 1992], but long-term modeling of three-dimensional thermal structure and circulation in the Great Lakes was virtually non-existent until the implementation of the Great Lakes Forecasting System (GLFS) in the early 1990s [*Bedford and Schwab*, 1990; *Schwab and Bedford*, 1994]. Currently, the GLFS does not provide information in winter (because of the lack of an ice model). Therefore winter and annual circulation patterns and their interannual variability remain poorly known.

Since the pioneering works of *Simons* [1974, 1975, 1976] and *Bennett* [1977] created the basis for numerical studies of circulation and thermal structure in the Great Lakes, Lake Michigan has been the subject of only two long-term modeling exercises: *Allender and Saylor* [1979] simulated the annual cycle of three-dimensional circulation and thermal structure, and

Schwab [1983] studied circulation with a two-dimensional barotropic model for an 8 month period. This is in sharp contrast with numerous attempts to simulate the ocean's climate in the past 2–3 decades [*Semtner*, 1995]. Recently, an opportunity to fill a gap in long-term modeling of currents and temperature in Lake Michigan presented itself within the framework of the U.S. Environmental Protection Agency (USEPA) Lake Michigan Mass Balance Study (LMMBS), whose primary goal is calculation of the mass budget of several toxic chemicals in the lake [*Schwab and Beletsky*, 1998]. In LMMBS the hydrodynamic model output is being used as input in sediment and contaminant transport models. An extensive array of measurements collected on Lake Michigan prior to and during the LMMBS field years provided an excellent data set for evaluation of numerical models.

The numerical model used here is a three-dimensional ocean circulation model (Princeton Ocean Model) developed for coastal ocean applications by *Blumberg and Mellor* [1987] and subsequently adapted for Great Lakes use at National Oceanic and Atmospheric Administration (NOAA) Great Lakes Environmental Research Laboratory [*Schwab and Bedford*, 1994; *O'Connor and Schwab*, 1994]. Extensive tests with observed currents, water level fluctuations, and surface temperature distributions have been carried out during the development of the GLFS [*Kuan et al.*, 1994] on Lake Erie. The model was also used for simulations of internal Kelvin waves in Lake Michigan [*Beletsky et al.*, 1997]. Recently, the Princeton Ocean Model has also been used for long-term coastal modeling in the Mediterranean Sea [*Zavatarelli and Mellor*, 1995] and the Gulf of Maine [*Xue et al.*, 2000].

The present study is focused on long-term modeling of Lake Michigan hydrodynamics. The results are presented in two separate papers. This paper is focused on the description of forcing functions, results of multiyear simulations of tempera-
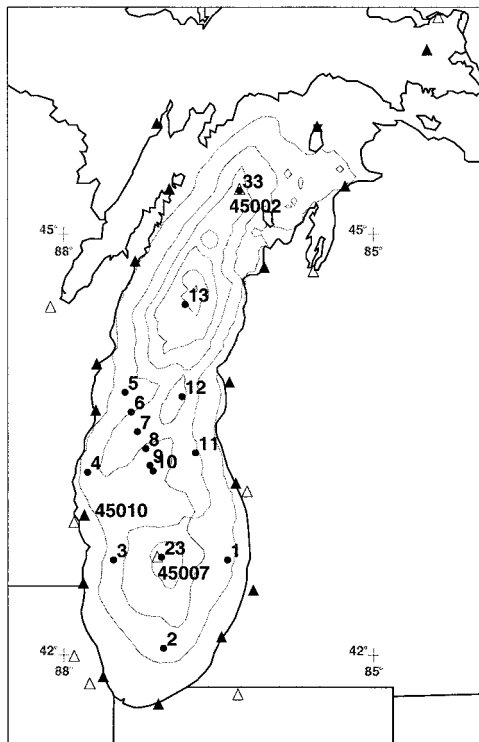
Figure 1. Observation network for 1982–1983 and 1994–1995: solid circles, current meters; open triangles, meteorological stations; and solid triangles, additional meteorological stations in 1994–1995. Isobaths are every 50 m.

ture and circulation patterns in Lake Michigan, and comparison with observations. It provides, for the first time, maps of modeled seasonal and annual circulation in Lake Michigan and thus makes a first step in developing a true climatology. Physical mechanisms responsible for observed long-term circulation patterns are investigated more fully in a companion paper (D. J. Schwab and D. Beletsky, manuscript in preparation, 2001). The Princeton model was applied to Lake Michigan for two 2 year periods: 1982–1983 and 1994–1995. The first 2 year period was chosen for the model calibration because of an extensive set of subsurface current and temperature data at 15 moorings (more details are given by *Gottlieb et al.* [1989]) along with surface temperature observations at two meteorological buoys (Figure 1). The second period, 1994–1995, is the field study period of LMMBS. During this period, conductivity-temperature-depth (CTD) survey data were available along with surface temperature observations at three buoys and solar radiation measurements at several locations. Although current measurements were also available at several locations, the coverage was not as comprehensive as in the 1982–1983 array [*Schwab and Beletsky*, 1998].

Under normal circumstances, multiyear modeling of Lake Michigan would require development of some sort of an ice model because the lake is partially covered with ice from December to April. Maximum ice extent is normally observed in late February to early March, when ice covers 45% of Lake Michigan [*Assel et al.*, 1983]. Fortunately, lack of an ice model was not a significant problem for the chosen periods of study: the 1982–1983 and 1994–1995 winters were among the warmest winters of the century and therefore practically ice-free [*Assel et al.*, 1985].

The outline of this paper is as follows. The hydrodynamic model is briefly described in section 2. A rather detailed description of the forcing functions is provided in section 3. Model results are presented in section 4 followed by comparison with observations in section 5. Discussion and conclusions are presented in section 6.

2. Hydrodynamic Model

The Princeton model of *Blumberg and Mellor* [1987] is a nonlinear, fully three-dimensional, primitive equation, finite difference model that solves the heat, mass, and momentum conservation equations of fluid dynamics. The model is hydrostatic and Boussinesq so that density variations are neglected except where they are multiplied by gravity in the buoyancy force. The model uses time-dependent wind stress and heat flux forcing at the surface, zero heat flux at the bottom, free-slip lateral boundary conditions, and quadratic bottom friction. The drag coefficient in the bottom friction formulation is spatially variable. It is calculated on the basis of the assumption of a logarithmic bottom boundary layer using a constant bottom roughness of 1 cm.

The model includes the *Mellor and Yamada* [1982] level 2.5 turbulence closure parameterization. The vertical mixing coefficients for momentum and heat are calculated from the variables describing the flow regime. The turbulence field is described by prognostic equations for the turbulence kinetic energy and turbulence length scale. Horizontal diffusion is calculated with a Smagorinsky eddy parameterization (with a multiplier $C = 0.1$) to give a greater horizontal mixing coefficient near strong horizontal gradients. Horizontal momentum diffusion is assumed to be equal to horizontal thermal diffusion, as is common practice in hydrodynamic models where the primary horizontal mixing process is eddy diffusion [*Blumberg*, 1986]. The equation of state [*Mellor*, 1991] calculates the density as a function of temperature, salinity, and pressure. For applications to the Great Lakes the salinity is set to a constant value of 0.2 parts per thousand.

The hydrodynamic model of Lake Michigan has 20 vertical levels and a uniform horizontal grid size of 5 km (Figure 2). The bathymetry was derived from the 2 km gridded bathymetric data compiled by *Schwab and Sellers* [1980]. The 5 km gridded depths are slightly smoothed by adjusting the depths to ensure that the relative depth change between adjacent grid squares is <0.5 while still preserving the volume of the original grid. There is no open boundary in the model, which means that we neglect the influence of tributaries and outflow through the Straits of Mackinac on large-scale lake circulation. In Lake Michigan the hydraulic flow is at least an order of magnitude smaller than typical wind-driven and density-driven currents. Vertical levels were spaced more closely in the upper 30 m of water and near the bottom to resolve better both the seasonal thermocline and bottom boundary layer (vertical levels at $\sigma = 0, -0.0227, -0.0454, -0.0681, -0.0908, -0.1135, -0.1362, -0.1589, -0.1816, -0.2043, -0.2270, -0.2724, -0.3405, -0.4313, -0.5448, -0.6810, -0.7945, -0.8853, -0.9534, -1$).

In the Princeton model, there is an option to allow a portion of the short-wave radiation to penetrate the upper part of the water column according to one of *Jerlov's* [1976] five optical categories ranging from I (lower light extinction) to III (higher light extinction). We found the results of the Lake Michigan model were rather insensitive to changes in the extinction
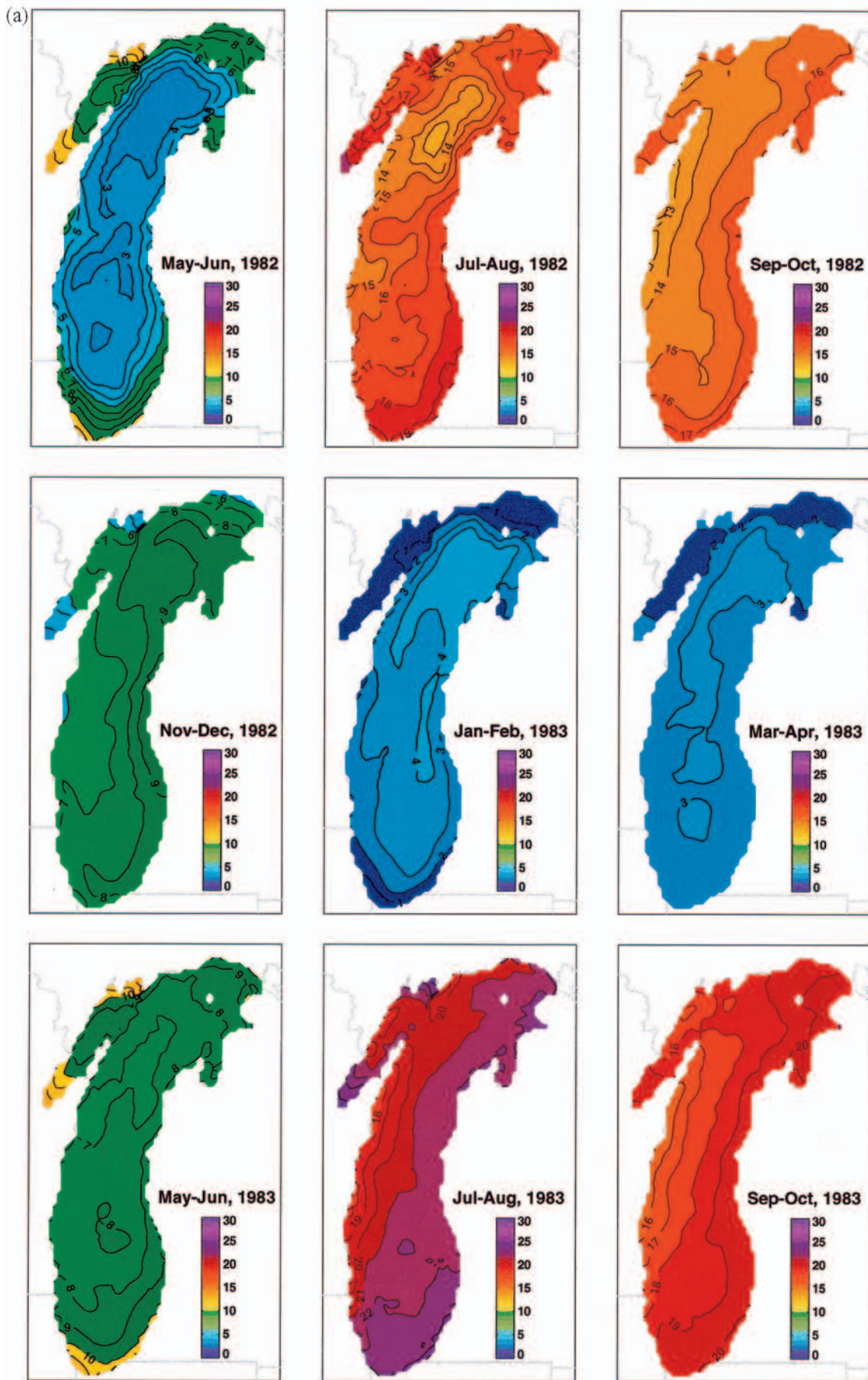
(a)

Plate 1. Bimonthly averaged lake surface temperature: (a) 1982–1983 and (b) 1994–1995.
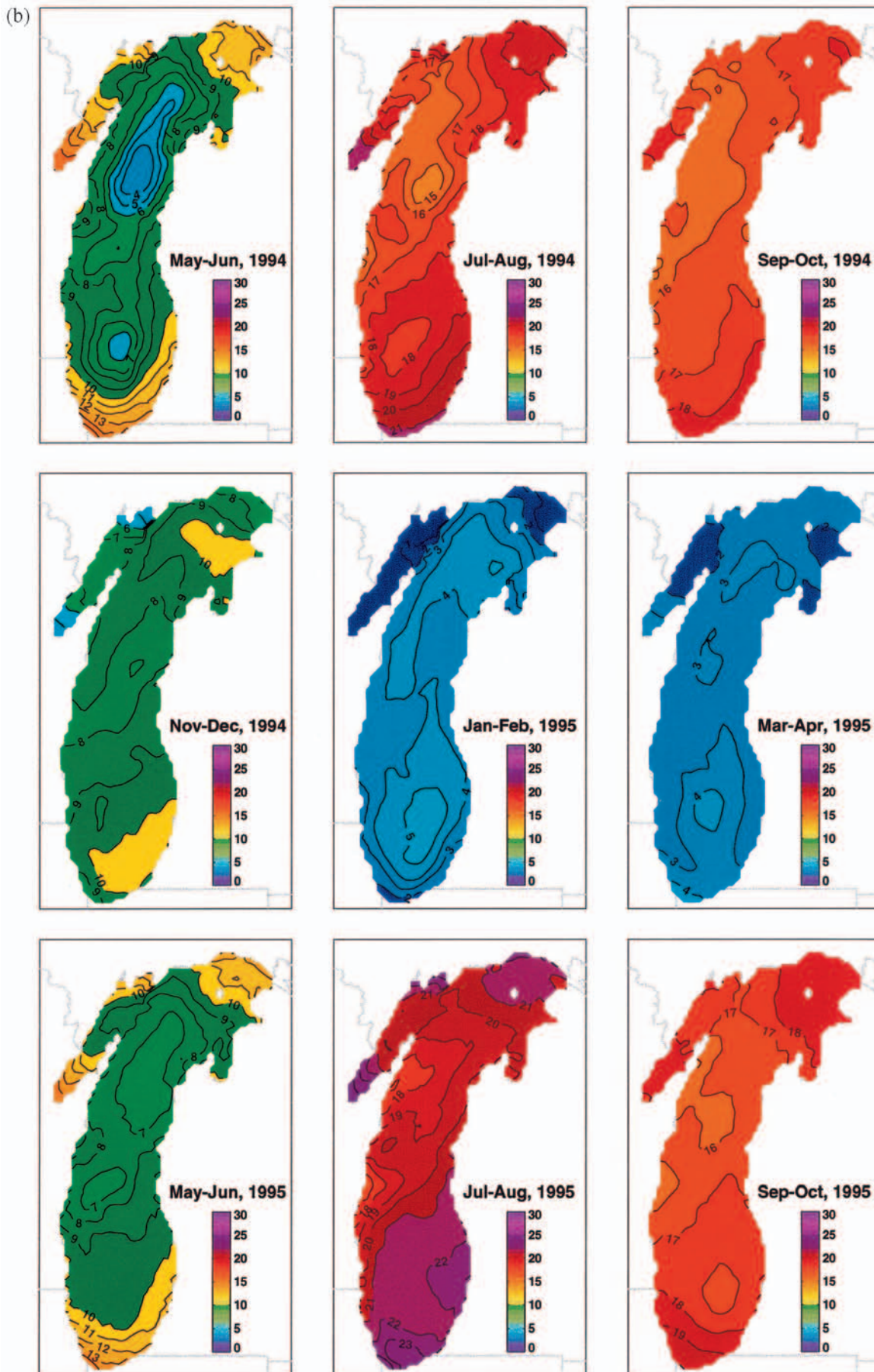
(b)
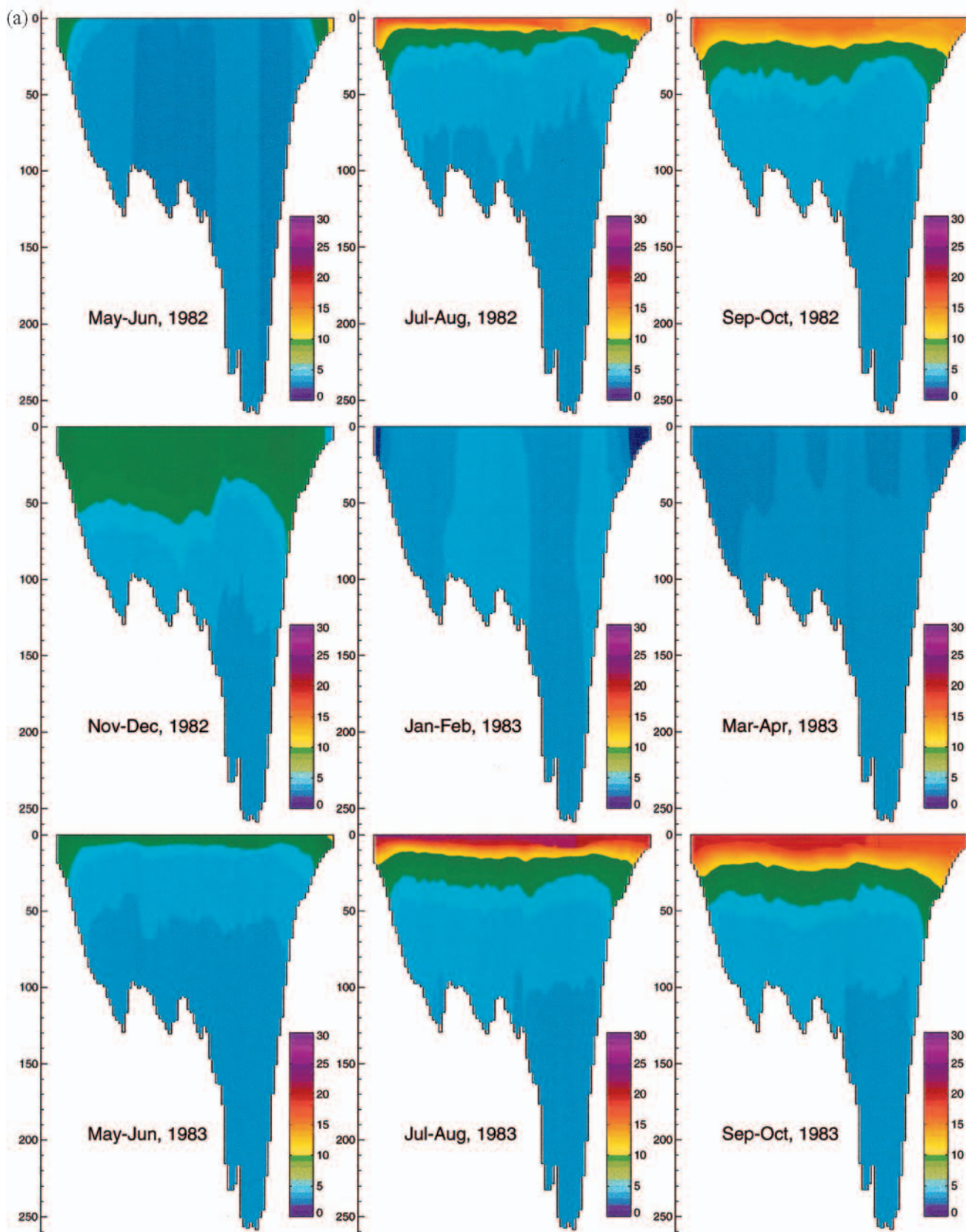
Plate 1. (continued)

Plate 2. Bimonthly averaged temperature at N-S transect in Figure 2 for (a) 1982–1983 and (b) 1994–1995.
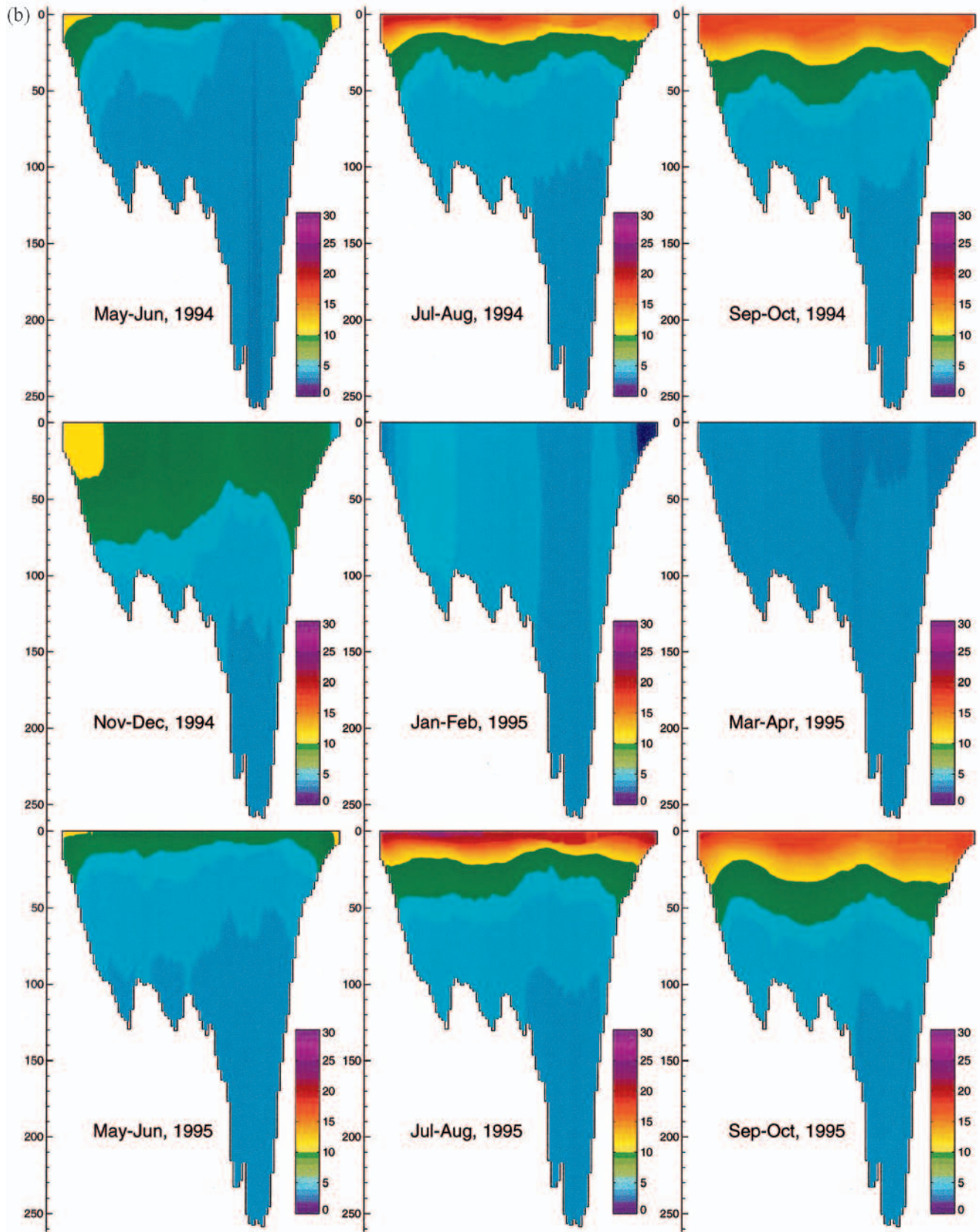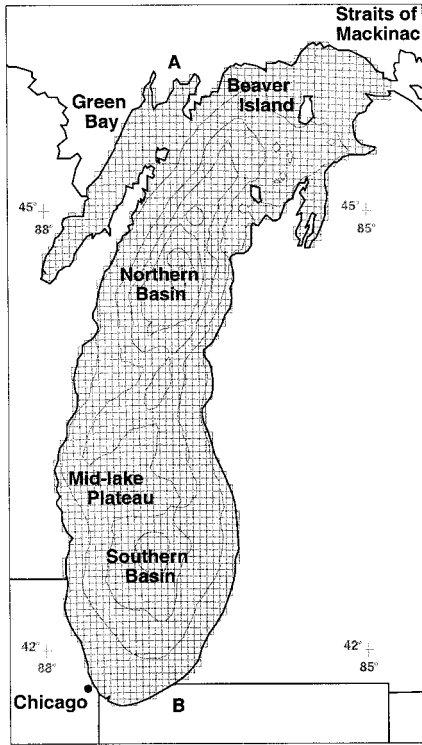
Plate 2.   (continued)

Figure 2. Lake Michigan bathymetry, model grid, and longitudinal cross-section AB used in Plate 2. Isobaths are every 50 m.

coefficient and therefore use Jerlov's optical category IA (default in the Princeton model). We also set a minimum water temperature in the model (0°C) to prevent negative water temperatures in winter due to the lack of an ice model. We felt that because ice cover in both winters was so low (maximum ice cover reached only 17% in 1982–1983 and 20% in 1994–1995), this procedure would have negligible effect on conservation of heat in the model.

3. Forcing Functions

We use a bulk aerodynamic formulation to calculate heat and momentum flux fields over the water surface for the lake circulation model for which it is necessary to estimate wind, temperature, dew point, and cloud cover fields at model grid points. Hourly meteorological data were obtained from the National Weather Service (NWS) stations and buoys as well as additional marine observations from U.S. Coast Guard stations and ships of opportunity in Lake Michigan. These data are routinely collected and quality controlled at the Cleveland Weather Service Forecast Office. In addition, data from several meteorological stations in the LMMBS air sampling network around Lake Michigan were used. The marine observation network is shown in Figure 1 (in 1982–1983 simulations, only NWS weather station and buoy data were available). These observations form the basis for generating gridded overwater wind, temperature, dew point, and cloud cover fields at hourly intervals.

3.1. Interpolation of Meteorological Data

Three main steps are required to develop overwater fields from the marine observation database: (1) height adjustments,

(2) overland/overlake adjustment, and (3) interpolation. First, measurements must be adjusted to a common anemometer height. Ship observations are usually obtained at considerably higher distances above the water surface than are buoy measurements. Measurements are adjusted to a common 10 m height above the water surface using profile methods developed by *Schwab* [1978] and described more thoroughly by *Liu and Schwab* [1987]. The wind and temperature profiles are represented as

$$u(z) = (u_*/k)[ln(z/z_0) - \Psi_m] \tag{1}$$

$$T_a(z) = T_0 + (T_*/k)[ln(z/z_0) - \Psi_h], \tag{2}$$

where u is wind speed, z is the vertical coordinate, u_* is friction velocity, $k = 0.4$ is the von Karman constant, T_a is air temperature, $T_0 = T_a(0)$ is the surface temperature, T_* is the scaling temperature, and Ψ_m and Ψ_h are functions of dimensionless stability height given by *Long and Shaffer* [1975]. In conjunction with the *Charnock* [1955] relation for overwater surface roughness, $z_0 = 0.045\ u_*^2/g$, these equations can be solved iteratively to obtain z_0 and u_*, yielding profiles for $u(z)$ and $T_a(z)$.

The second problem in dealing with the combination of overland and overwater measurements is that overland wind speeds generally underestimate overwater values because of the marked transition from higher aerodynamic roughness over land to much lower aerodynamic roughness over water. This transition can be very abrupt so that wind speeds reported at coastal stations are often not representative of conditions only a few kilometers offshore. *Schwab and Morton* [1984] found that wind speeds from overland stations could be adjusted by empirical methods to obtain fair agreement with overlake wind speeds measured from an array of meteorological buoys in Lake Erie. For meterological stations that are more representative of overland than overwater conditions, namely, airports and other "surface stations" in the marine observation network (Figure 1), we apply the empirical overland-overlake wind speed adjustment from *Resio and Vincent* [1977]. For wind speed this adjustment is

$$u_w = u_l F_1(u_l)\,F_2(\Delta T), \tag{3}$$

where $F_1(u_l) = 1.2 + 1.85/\,u_l$ (m s^{-1}), $F_2 = 1 - (\Delta T/|\Delta T|)(|\Delta T|/1920)^{1/3}$, u_w is the over water wind speed, u_l is overland wind speed, and $\Delta T = T_a - T_w$ (°C).

For heat flux calculations we also need to know overwater humidity to calculate latent heat flux. Dew point observations are only available from land stations. *Phillips and Irbe* [1978] used a simple empirical formula to estimate overwater dew point temperature from overland values:

$$T_{dw} = T_{dl} - c_1(T_{dl} - T_w), \tag{4}$$

where T_{dw} is the dew point temperature over water, T_{dl} is the dew point temperature over land, and c_1 is on the order of 0.35 for neutral stability. Air temperature reports from overland stations are adjusted with a similar empirical formula:

$$T_a = 0.4T_{al} + 0.6T_w, \tag{5}$$

where T_a is the air temperature over water, T_{al} is the air temperature over land, and T_w is lake-averaged surface water temperature.

Finally, in order to interpolate meteorological data observed at irregular points in time and space to a regular grid, some

type of objective analysis technique must be used. The complexity of the analysis technique should be compatible with the complexity of the observed data; that is, if observations from only a few stations are available, a best fit linear variation of wind components in space might be an appropriate method. If more observations can be incorporated into the analysis, spatial weighting techniques can be used. For LMMBS we used the nearest neighbor technique, with the addition of a spatial smoothing step (with a specified smoothing radius). The nearest neighbor technique assigns the value of the nearest measurement station to each point in the regular grid, similar to the Thiessen polygon weighting scheme [*Thiessen*, 1911]. The spatial smoothing step replaces each value on the regular grid with the average of all grid points within the specified smoothing radius. In the nearest neighbor technique we also consider observations from up to 3 hours before the interpolation time to 3 hours after the interpolation time. In the nearest neighbor distance calculations the distance from a grid point to these observation points is increased by the product of the time difference multiplied by a scaling speed. The interpolation scaling speed is taken as 10 km hr^{-1}. The interpolation smoothing distance is 30 km. We found that the nearest neighbor technique provided results comparable to results from the inverse power law or negative exponential weighing functions.

Figures 3a–3b show time series of spatially averaged air temperature during 600 days (roughly from April of the first year until November of the second year) in 1982–1983 and 1994–1995 generated by this procedure. This period includes two periods of lake stratification separated by a nonstratified period. Figures 3a–3b show a pronounced seasonal cycle with relatively mild winter temperatures. The mean regional temperature anomaly reached 3.6°C above normal in December 1982 to February 1983 and 1.9°C in December 1994 to February 1995. Maximum temperatures were also higher in the second summer (~24°C compared with 21°C in the first summer). This tendency is also noticeable in surface water temperatures (based on modeled temperatures in 1982–1983 and satellite-derived temperatures in 1994–1995).

3.2. Momentum Flux

To calculate momentum flux, the profile theory described above [*Liu and Schwab*, 1987] for anemometer height adjustment is used at each grid square at each time step to estimate surface stress, using the surface water temperature from the circulation model. This procedure provides estimates of bulk aerodynamic transfer coefficients for momentum and heat, which depend on the stability of atmospheric boundary layer. The stability is at its maximum in late spring-summer when air temperature is higher than water temperature and at minimum in fall-winter when water temperature is warmer. Figure 3 illustrates this tendency in both years with temperature differences reaching 10°C during some episodes in winter and 6°C in summer. Wind stress also has a pronounced seasonal cycle with maximum stresses occurring in late fall to early spring (strong winds, minimum stability) and minimum stresses in summer (weak winds, maximum stability). Equally strong zonal and meridional winds were present during episodic events. At the same time, significant interannual variability is evident: spring storms in 1982 with maximum wind stress reaching 6.8 dyn cm^{-2} were stronger than storms in 1983 and 1994–1995, while winter storms in the late fall of 1995 with maximum wind stress reaching 7.2 dyn cm^{-2} were noticeably stronger than those of 1994 or 1982–1983.

Figures 4a–4b show wind stress patterns over 18 months in 1982–1983 and 1994–1995 to illustrate seasonal variability in wind stress direction. An explanation of time-averaging scales is due here. As earlier observations of lake currents indicated, they are very sensitive to wind forcing. Typically, mean currents are an order of magnitude smaller than instantaneous currents with effects of individual storms sometimes seen in monthly averages. Therefore we present most of our results (wind stress, currents, and temperature) in the form of bimonthly averages in order to provide a more reliable description of seasonal changes. During November–December the wind stress was W–SW. It changed its direction to NW in January–February and to NE in March–April. Northerly wind stress continued to dominate in May–June but reversed its direction in July–August to become SW, which also held for September–October. Both cyclonic and anticyclonic vorticity were present in the wind stress fields. Particularly strong cyclonic vorticity in the wind stress field was observed in winter and spring months: January–February 1983 and March–April 1995.

3.3. Heat Flux

Surface heat flux H is calculated as

$$H = H_{sr} + H_s + H_l + H_{lr}, \tag{6}$$

where H_{sr} is short-wave radiation from the Sun, H_s is sensible heat transfer, H_l is latent heat transfer, and H_{lr} is long-wave radiation. The heat flux procedure follows the methods described by *McCormick and Meadows* [1988] for mixed layer modeling in the Great Lakes. H_{sr} is calculated on the basis of latitude and longitude of the grid square, time of day, day of year, and cloud cover (CL).

$$H_{sr} = H_{cs}F_3(CL), \tag{7}$$

where H_{cs} is a clear-sky value and F_3 is a cubic function of cloud cover that ranges from 1.0 for clear sky to 0.36 for total cloud cover. H_s and H_l are calculated using the bulk aerodynamic transfer formulas:

$$H_s = C_h C_p \rho_a u_w \Delta T \tag{8}$$

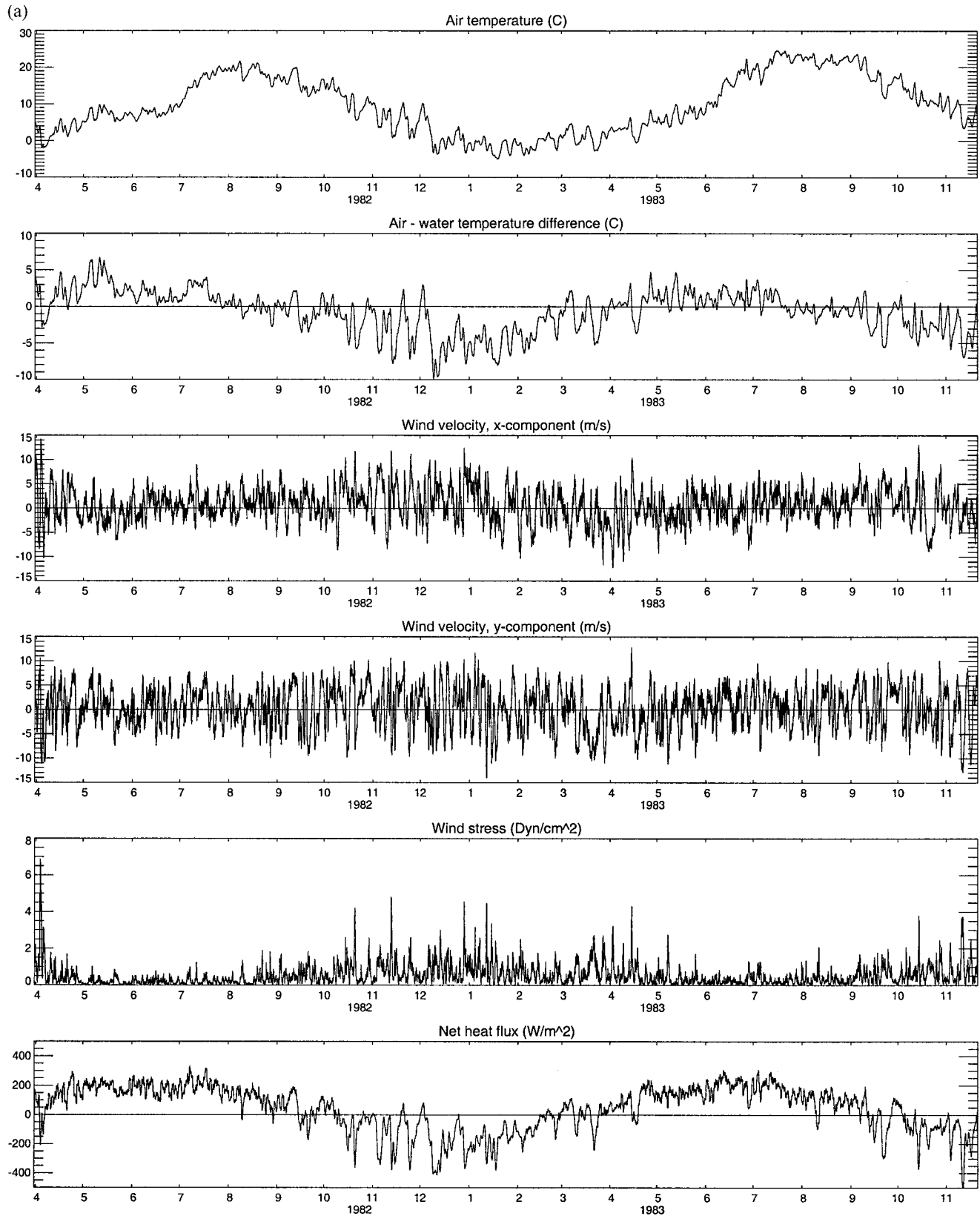$$H_l = C_d q_l \rho_a u_w (h_a - h_w), \tag{9}$$

where C_h is the bulk heat coefficient, C_p is the specific heat of air at constant pressure, ΔT is the water-air temperature difference, C_d is the drag coefficient, q_l is the latent heat of vaporization, h_a is the specific humidity of air, and h_w is specific humidity at the water surface. H_{lr} is calculated as a function of T_a, T, and cloud cover according to *Wyrtki* [1965]. *McCormick and Meadows* [1988] showed that this procedure works quite well for modeling mixed layer depth in the Great Lakes.

The annual cycles of the net heat flux in 1982–1983 and 1994–1995 are shown in Figure 3a and Figure 3b, respectively. The range is from ~−200 W m^{-2} in winter to 200 W m^{-2} in summer. Significant nearshore-offshore gradients of the net heat flux develop mostly in spring and winter. These are periods of intense lake warming (cooling) during which deep offshore areas absorb (release) more heat than shallow coastal areas. In addition, strong gradients also exist in summer and fall in areas of wind-induced upwelling along the west coast.

4. Model Results

The baroclinic model runs start in April of 1982 (1994) to avoid problems with initialization of the water temperature

(a)

Air temperature (C)

Air - water temperature difference (C)

Wind velocity, x-component (m/s)

Wind velocity, y-component (m/s)

Wind stress (Dyn/cm^2)

Net heat flux (W/m^2)

Figure 3. Time series of spatially averaged meteorological parameters for (a) 1982–1983 and (b) 1994–1995. Temperature and heat flux data are 24 hour smoothed.
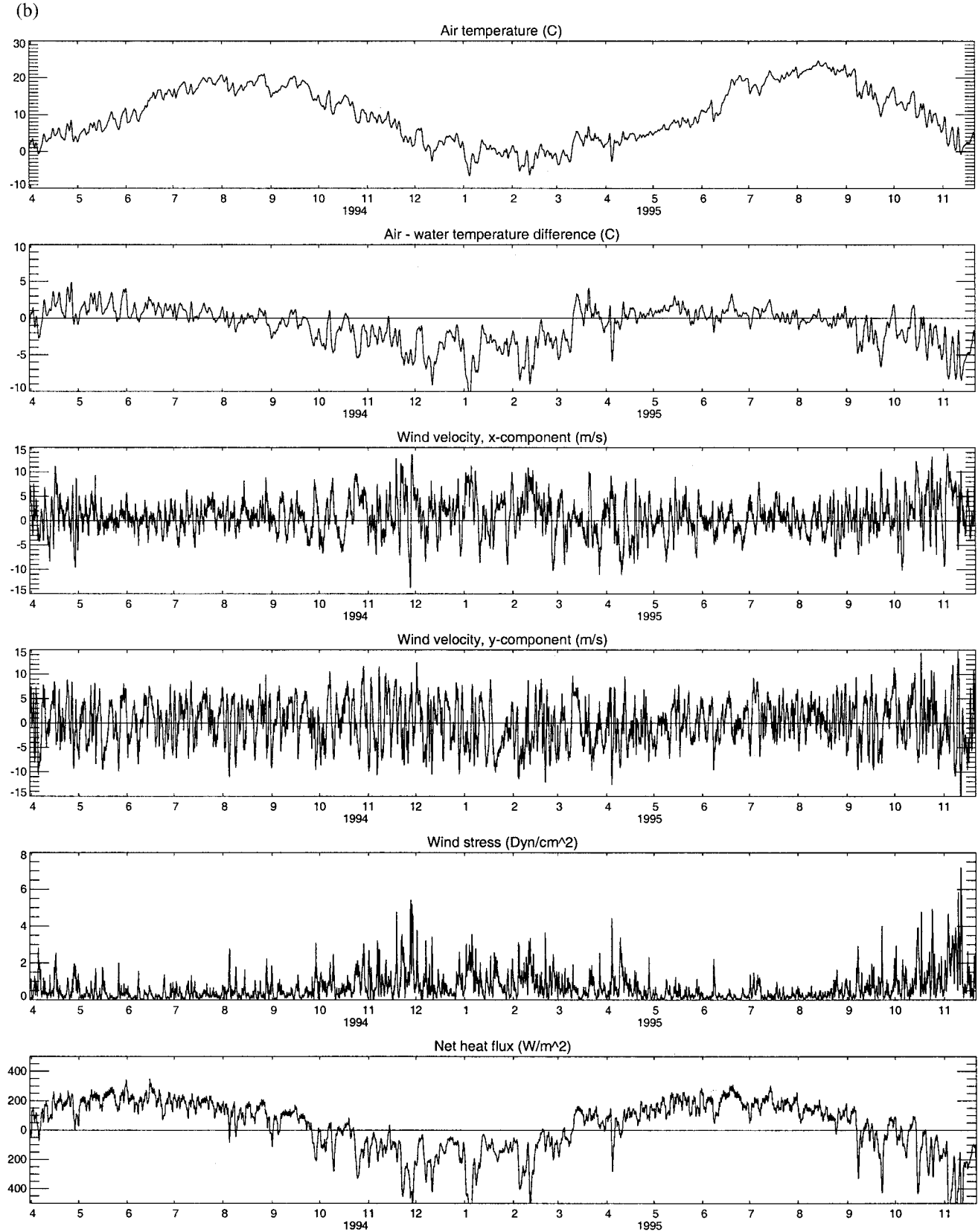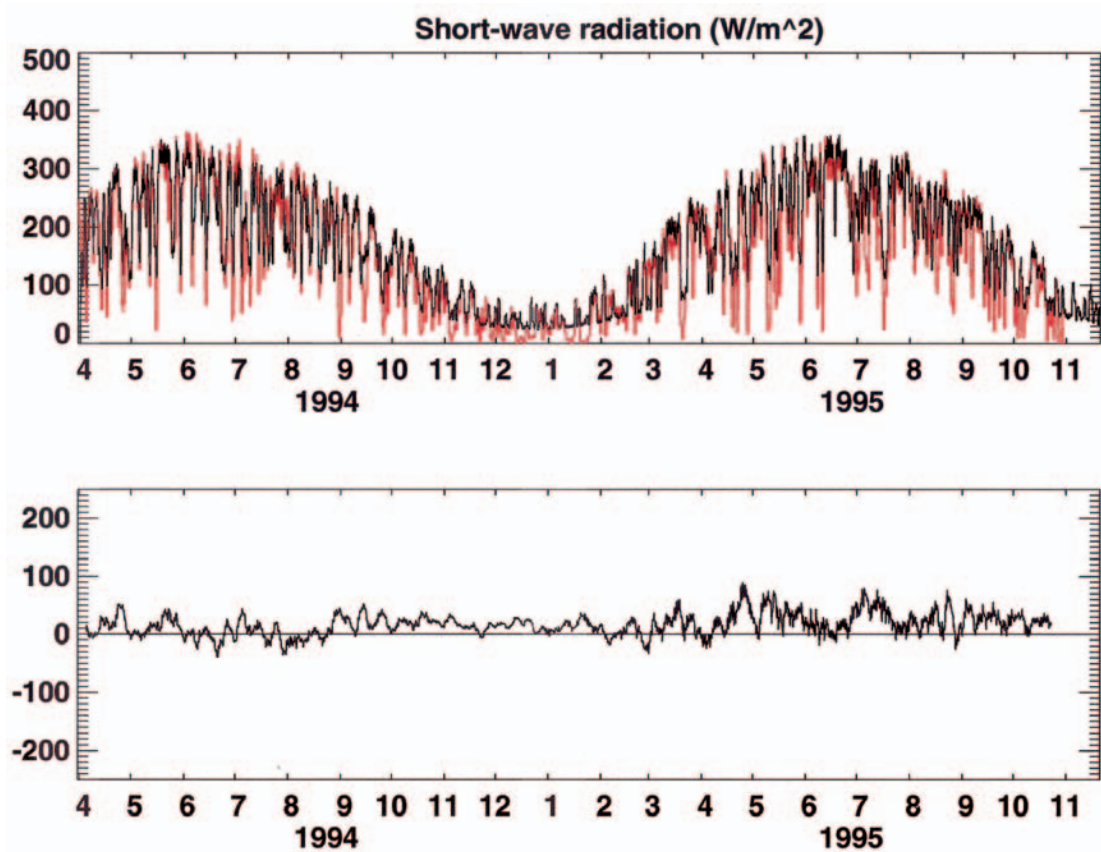
(b)

Air temperature (C)

Air - water temperature difference (C)

Wind velocity, x-component (m/s)

Wind velocity, y-component (m/s)

Wind stress (Dyn/cm^2)

Net heat flux (W/m^2)

Figure 3. (continued)

Plate 3. (top) Simulated (black line) versus observed (red line) short-wave radiation (in W m^{-2}) in 1994–1995 at Beaver Island. Both are smoothed with a 24 hour filter. (bottom) Their difference smoothed with a 120 hour filter.
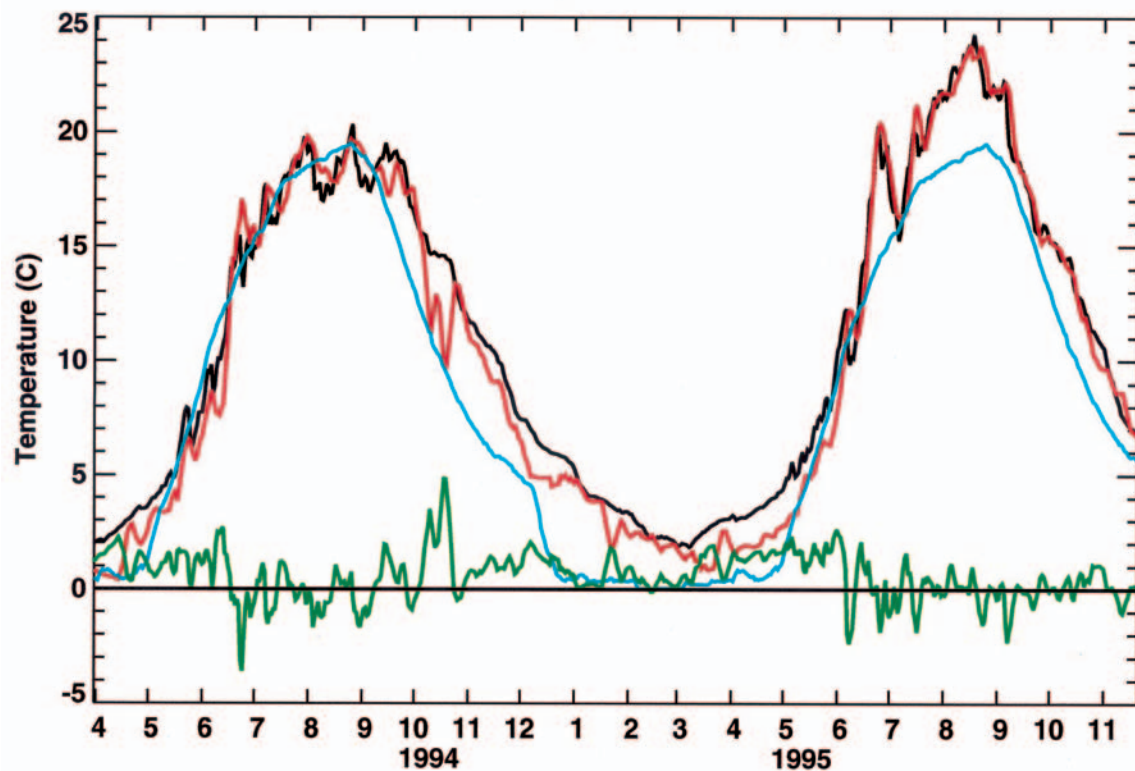
Plate 4. Time series of climatological (blue line), observed (red line), and modeled (black line) lake surface temperature in 1994–1995. Green line represents the difference between modeled and observed temperature.
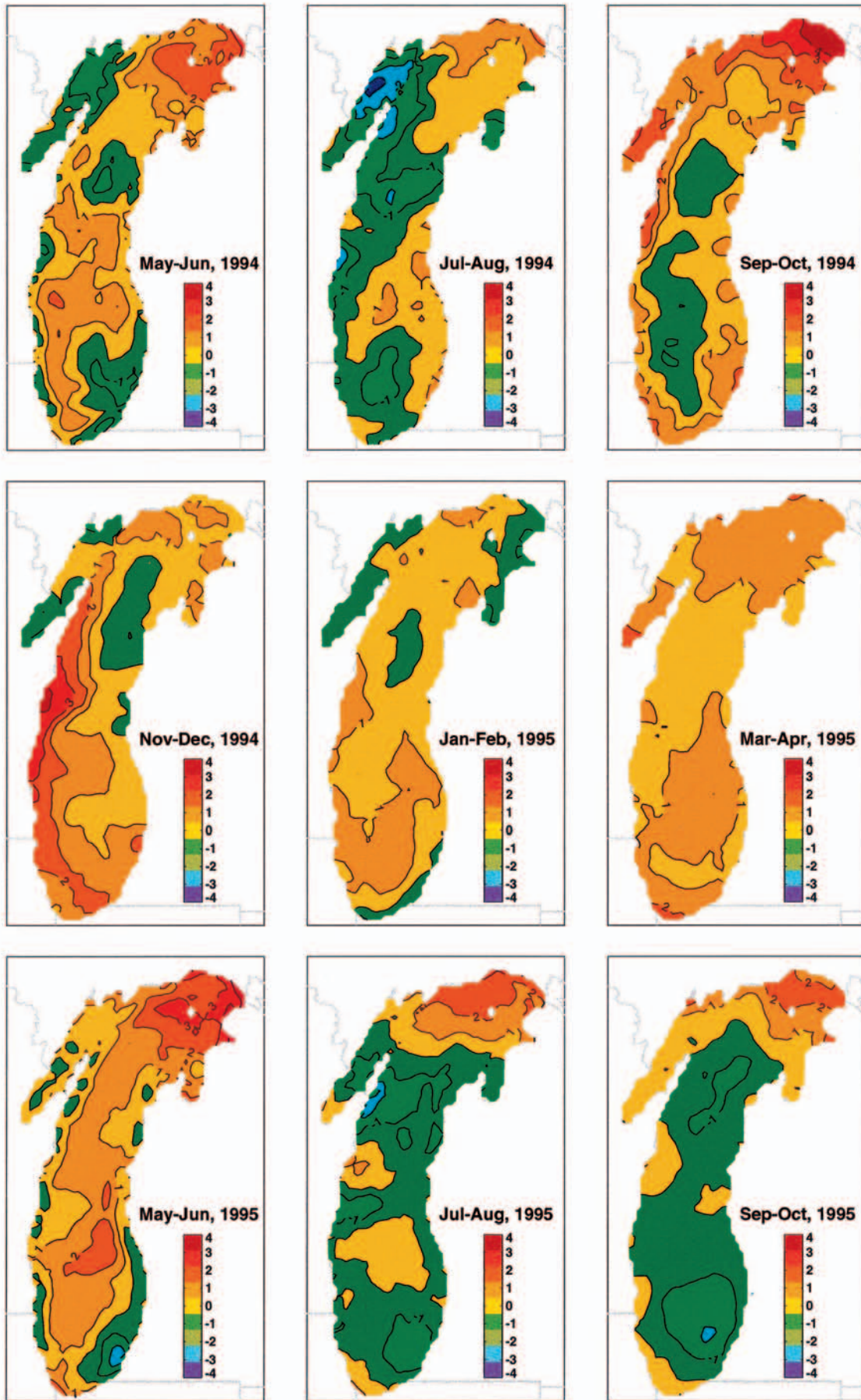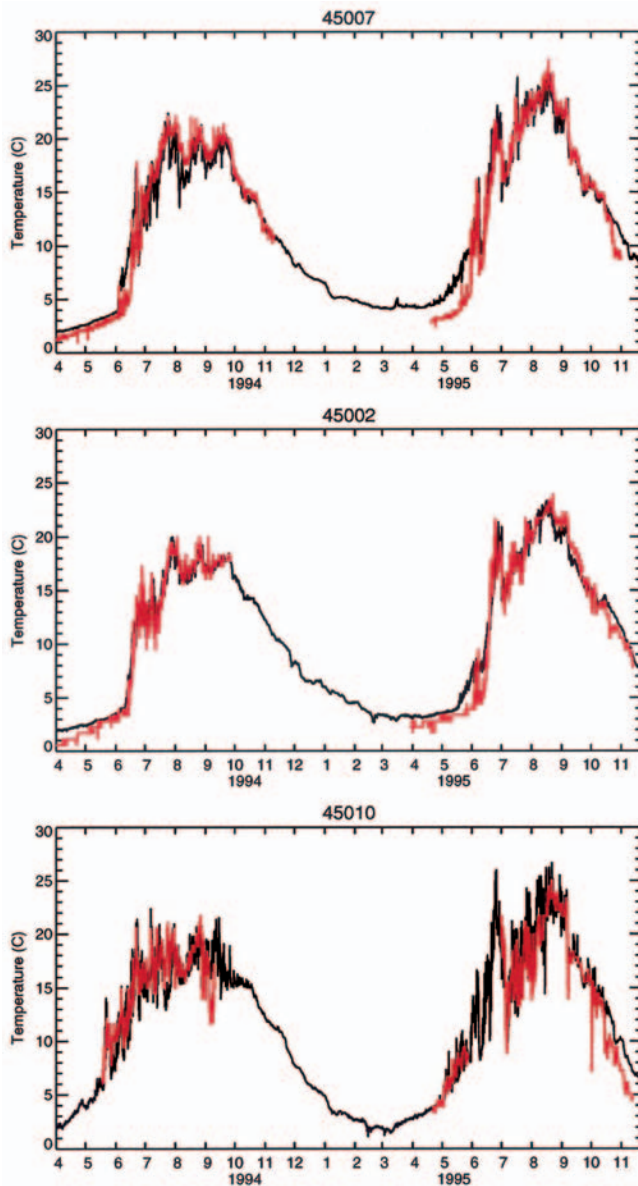
Plate 5.   Bimonthly averaged difference between modeled and observed lake surface temperature in 1994–1995.

Plate 6. Time series of simulated (black line) surface water temperature versus observed (red line) at 45007, 45002, and 45010 in 1994–1995.

field during significant ice cover in January-March. In particular, the first 3 months of 1982 and 1994 would be most challenging for modeling because of the extensive ice cover, which reached 65% during the winter of 1981–1982 and 83% during the winter of 1993–1994 [*Assel et al.*, 1996]. All model runs end in late fall (November–December) of the second year. Because of the strongly wind-driven character of the circulation in the lake the spin-up time is very short. The effect of the initial condition for velocity on calculated currents disappears within the first few weeks of the simulation or even the first few days if there is a strong wind event.

To initialize the temperature field in the model, we used surface temperature observations at two buoys (45007 and 45002) located near the centers of the southern and northern halves of the lake, respectively. Vertical temperature gradients are very small in early spring because of convection during that time of the year. The typical range of water temperature in

Lake Michigan for that time of year is from 0 to 3°C, less than the temperature of maximum density (4°C). Extensive experiments with different initial conditions for the 1994–1995 period revealed that statistically, model results were insensitive to the prescribed initial temperature conditions (necessarily simplified because of insufficient observations) if the mean lake temperature difference between different model runs was within ~0.5°–1°C. After allowing model currents to spin up for 1 month we present results from May of the first year until October of the second year (18 months). This period covers 6 months of thermal stratification of the first year followed by 6 months of relatively homogeneous conditions (in winter) and another 6 months of stratification during the second year.

4.1. Temperature

The most distinctive feature of the physical limnology of the Great Lakes is a pronounced annual thermal cycle [*Boyce et al.*, 1989], which also presents the most challenging situation for modeling since the lake changes from entirely thermally mixed in winter to strongly stratified in summer. Nevertheless, the model was able to reproduce all of the basic features of the thermal structure evolution in Lake Michigan (Plates 1 and 2). In the beginning of spring, Lake Michigan becomes well mixed from top to bottom at temperatures near or below the temperature of maximum density for freshwater, about 4°C. This is well illustrated by the vertical temperature distribution in March–April in both 1983 (Plate 2a) and 1995 (Plate 2b). Springtime warming tends to heat and stratify shallower areas first, leaving a pool of cold water (<4°C and vertically well mixed because of convection) in the deeper parts of the lake. In spring, stratified and homogeneous areas of the lake are separated by a sharp thermal front, commonly known as the thermal bar. This front is clearly seen in May–June 1982 (Plate 1a) and in May–June 1994 (Plate 1b). Depending on meteorological conditions and the depth of the lake, the thermal bar may last for a period of from 1 to 3 months. Thus, in May–June 1994 the front had propagated across almost the entire lake (Plate 2b), while in 1982 it had only begun its offshore movement (Plate 2a). Stratification eventually covers the entire lake, and a well-developed thermocline generally persists throughout the summer. Wind-induced upwellings along the west coast of Lake Michigan are typical for this time of the year. Figures 4a and 4b illustrate upwelling favorable SW winds in July–August and September–October.

In the fall, decreased heating and stronger vertical mixing tend to deepen the thermocline until the water column is again mixed from top to bottom. When the nearshore surface temperature falls below the temperature of maximum density, the fall–winter thermal bar starts its propagation from the shoreline toward the deeper parts of the lake (January–February panels in Plates 1a, 1b, 2a, and 2b). Thermal gradients are much smaller during this period than during the springtime thermal bar. Further cooling during winter can lead to inverse stratification and ice cover. The fall–winter thermal bar in 1982–1983 and 1994–1995 was almost absent since both winters were very mild, and water temperature was above normal and close to the temperature of maximum density (4°C). The result of this thermal preconditioning was a weaker thermal bar in the spring of 1983 and 1995 than during previous springs. For example, the thermal bar front is entirely missing (also, in part, because of averaging) in the May–June 1983 panels of Plates 1a and 2a and in the May–June 1995 panels of

(a)
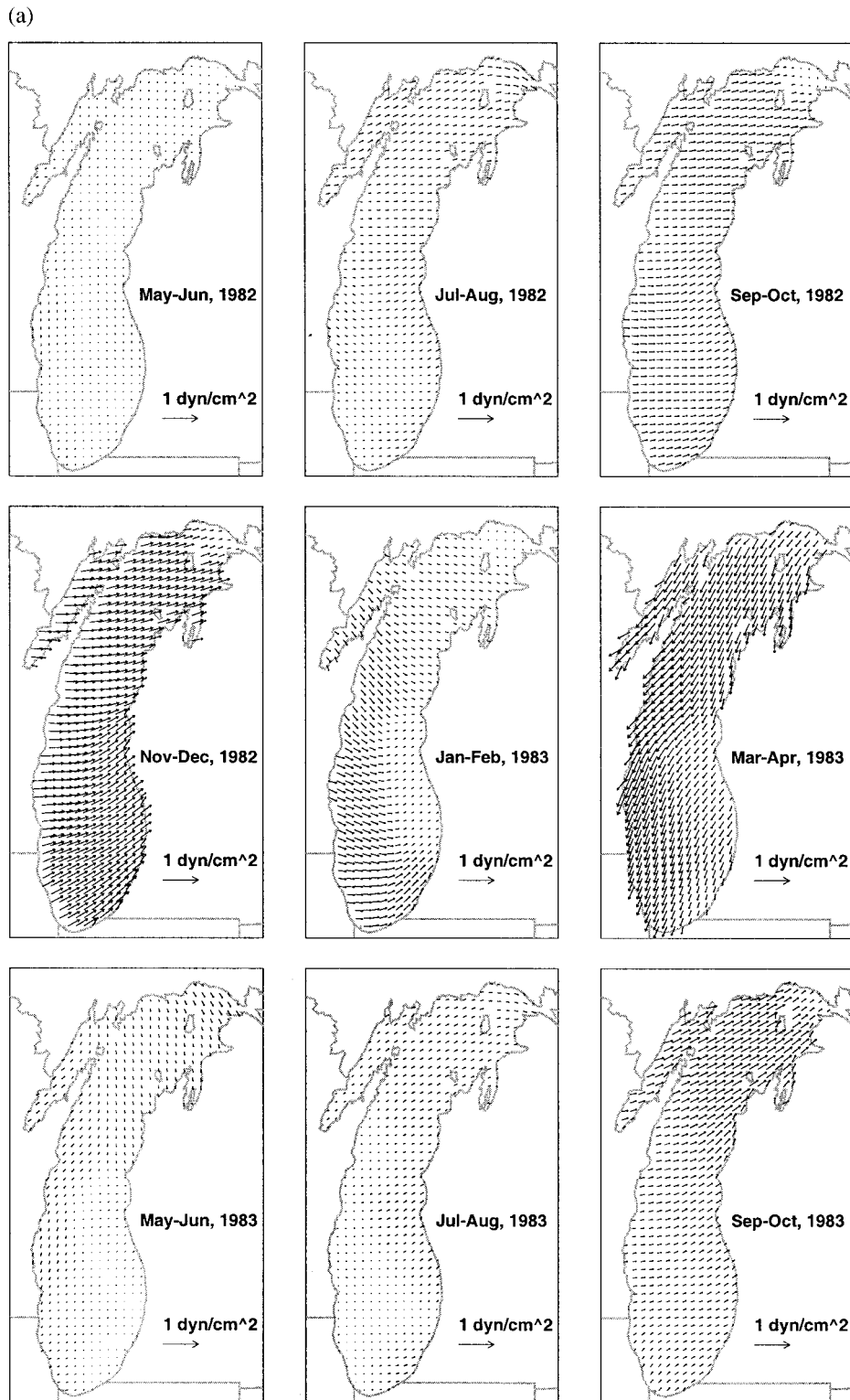
Figure 4.   Bimonthly averaged wind stress field: (a) 1982–1983 and (b) 1994–1995.

Plates 1b and 2b. Surface temperatures were significantly higher during the following summer.

4.2. Currents

Bimonthly plots of depth-averaged circulation showed stronger currents in winter than in summer (Figure 5), which is consistent with the seasonal changes in the wind field (Figures 3 and 4). This is because wind-driven transport is a dominant feature of circulation in large lakes. As shown by *Bennett* [1974], *Csanady* [1982], and others, the response of an enclosed basin with a sloping bottom to a uniform wind stress consists of longshore, downwind currents in shallow water and a net up-
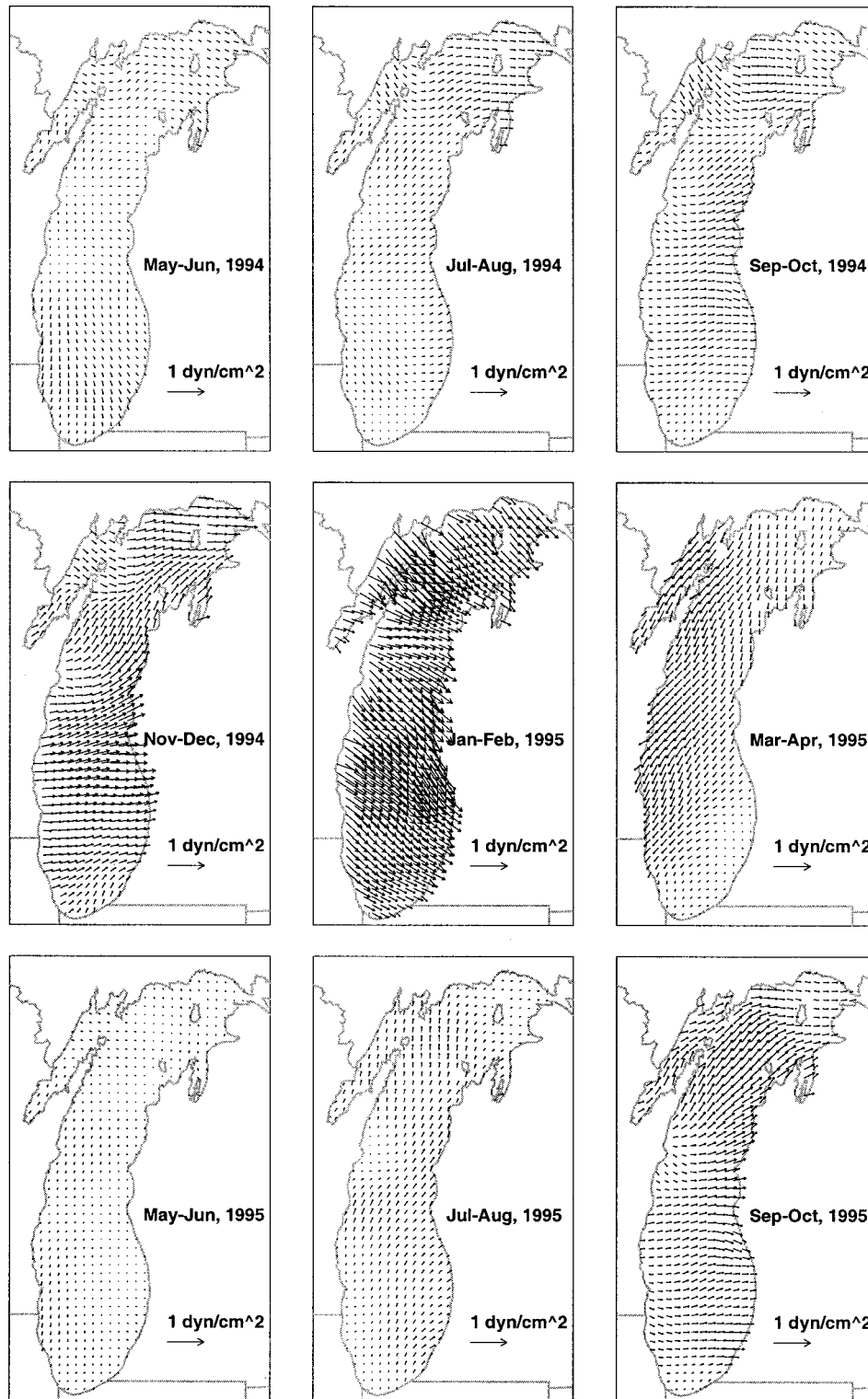
(b)

Figure 4. (continued)

wind return flow in deeper water. The streamlines of the flow field form two counterrotating closed gyres, a cyclonic gyre to the right of the wind and an anticyclonic gyre to the left (in the Northern Hemisphere). The results of these modeling exercises also show that the actual bathymetry of each of the Great Lakes tends to act as a combination of bowl-shaped subbasins, each of which supports its own two-gyre circulation pattern when wind-driven circulation is dominant. Nearshore currents are generally stronger than offshore currents.

Besides bathymetry and geometry, two other important fac-

tors are known to modify the simple two-gyre lake circulation model described above, namely, nonuniform wind forcing and stratification. Thus, during the stratified period, longshore currents frequently form a single-gyre cyclonic circulation pattern driven by onshore-offshore density gradients [*Schwab et al.*, 1995]. The effect of horizontal variability in the wind field enters through the curl of the wind stress field [*Rao and Murty*, 1970]. Any vorticity in the forcing field is manifest as a tendency of the resulting circulation pattern toward a single gyre streamline pattern, with the sense of rotation corresponding to the sense of rotation of the wind stress curl. Because of the size of the lakes, and their considerable heat capacity, it is not uncommon to see lake-induced mesoscale circulation systems superimposed on the regional meteorological flow, a mesohigh in the summer [*Lyons*, 1971] and a mesolow in the winter [*Pettersen and Calabrese*, 1959]. There are also indications that nonlinear interactions of topographic waves can contribute to the mean single-gyre cyclonic circulation [*Simons*, 1985].

Storm-induced currents in the Great Lakes can be quite strong (up to several tens of cm s^{-1}), but the average currents are relatively weak throughout most seasons of the year (of the order of only a few cm s^{-1}). Thus average bimonthly currents from April through October were only 0.6–1.4 cm s^{-1} with maximum speeds reaching 2.5–7.1 cm s^{-1}. During the November–March period, average bimonthly currents increased to 1.6–2.2 cm s^{-1} with maximum speeds up to 7.9–11.7 cm s^{-1}.

Circulation during 1982–1983 and 1994–1995 was mostly cyclonic, sometimes with pronounced separate cyclonic gyres in the northern and southern basins. Circulation in northern Green Bay is a notable exception. It was anticyclonic all the time except March–April of 1982. Besides seasonal variations in overall current speed, another important feature of Lake Michigan variability is variations of current vorticity, with minimum cyclonic vorticity in summer and maximum cyclonic vorticity in winter. Summer currents show more vertical structure than winter currents, especially on subinertial timescales, because of strong inertia-gravity waves. On the longer timescales, density-driven currents (mostly due to nearshore-offshore temperature gradients) contribute to vertical shear through the thermal wind relationship.

In May–June, circulation is weak overall, but the southern basin cyclonic gyre is more pronounced than the northern basin gyre because of earlier development of stratification. In July–August and September–October, circulation gradually becomes stronger with both cyclonic gyres being equally strong. The strongest circulation is observed when the lake is not stratified: from November until April. Circulation also looks more organized in winter than in summer.

Bimonthly currents exhibit significant interannual variability. The most dramatic example is a case of a typical cyclonic gyre in the southern basin being replaced by an anticyclonic gyre in November–December 1994. The origin of this anticyclonic gyre can probably be traced back to anticyclonic vorticity in the wind stress field in the southern basin (Figure 4b). Another example from the southern basin is a strong anticyclonic current off Chicago in September–October 1983 and 1994. In the northern basin (western part) a rather unusual anticyclonic circulation was observed in May–June 1994. Other examples of interannual variability include variations in strength of currents in the Beaver Island and in the midlake plateau areas.

To study changes in circulation patterns on longer than bimonthly timescales, we averaged model results over 6 and 12

month periods (Figure 6). The two 6 month periods roughly correspond to the stratified period (May to October, "summer") and nonstratified (November to April, "winter") period (Plate 2). A similar type of averaging was adopted previously for Great Lakes circulation studies by *Beletsky et al.* [1999a]. Averaging over 6 month periods reveals the existence of rather stable circulation patterns in Lake Michigan. Average 6 month current speed also exhibited significantly less variability when compared to bimonthly currents. Thus, during summer months the average current speed was 0.8–0.9 cm s^{-1} with maximum speed reaching 4.0–4.6 cm s^{-1}. During winter the average speed increased to 1.5–1.7 cm s^{-1} with maximum speed up to 7.1–7.4 cm s^{-1}. Annual current speed was also very consistent: average speed was 1.1–1.2 cm s^{-1} with maximum speed up to 5.3–5.7 cm s^{-1}.

Mean winter circulation (with strong coastal currents) was stronger and more cyclonic than summer circulation. The southern basin cyclonic gyre was somewhat less pronounced in 1995 than in 1983, probably as a consequence of anticyclonic circulation in November–December 1994. Anticyclonic circulation in the Beaver Island area and currents in the midlake plateau region were more energetic in 1995 winter than in 1983. In general, summer circulation was more variable than winter circulation, although it was very similar in 1994 and 1995. In 1983 an anticyclonic gyre was present off Chicago, while in 1982, summer currents along the west shore were significantly weaker than currents along the east shore. Annual circulation patterns were very similar in both years, resembling winter circulation patterns. The annual circulation was slightly stronger overall in 1982–1983, while circulation in the midlake plateau area was stronger in 1994–1995 with a pronounced anticyclonic gyre.

5. Comparison With Observations

A considerable number of current, temperature, and heat flux measurements were available for model evaluation during 1982–1983 and 1994–1995. We present some of the more comprehensive current meter records here, while the complete model/observation comparison is given by *Schwab and Beletsky* [1998].

5.1. Short-Wave Radiation

Accurate calculation of solar radiation is crucial for long-term temperature simulations in the lake because it is a dominant component of the net heat flux during most of the year. Within the framework of LMMBS, solar radiation measurements at several Illinois State Water Survey (ISWS) stations were available for comparison with calculated solar radiation. One of the stations was located on Beaver Island (Figure 2). That comparison showed good agreement between measured and calculated short-wave radiation (Plate 3), although the model overestimated short-wave radiation by 10–15%. Indirectly, the favorable comparison also indicates that the cloud parameterization scheme in the heat flux submodel worked reasonably well.

5.2. Temperature

Spatially averaged modeled surface temperature in 1994–95 was compared to remotely sensed temperature (Plate 4). The data are a product of the NOAA CoastWatch program [*Schwab et al.*, 1999]. Climatological temperatures from *Schneider et al.* [1993] are also shown to illustrate positive

(a)
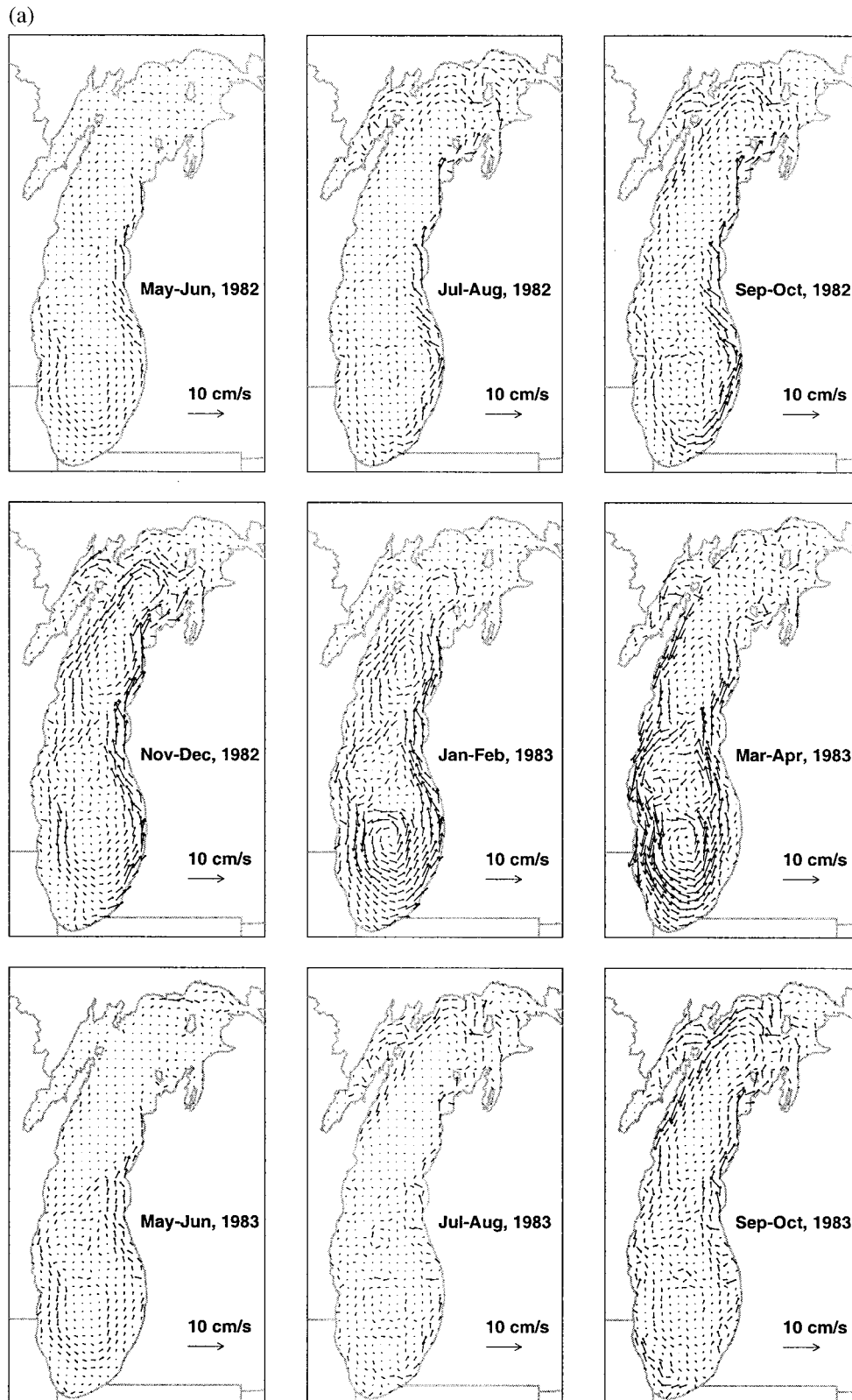
Figure 5. Bimonthly averaged depth-averaged currents: (a) 1982–1983 and (b) 1994–1995.

temperature anomalies during 1994–1995 winter and 1995 summer. Overall, the comparison is very good (the rms difference is 1.4°C, which shows correct calculation of heat fluxes near the surface), although the modeled temperature is warmer than the observed temperature in winter and colder than the observed temperature in summer. This tendency can also be seen in Plate 5, which provides details of the spatial distribution of differences between modeled and observed sur-
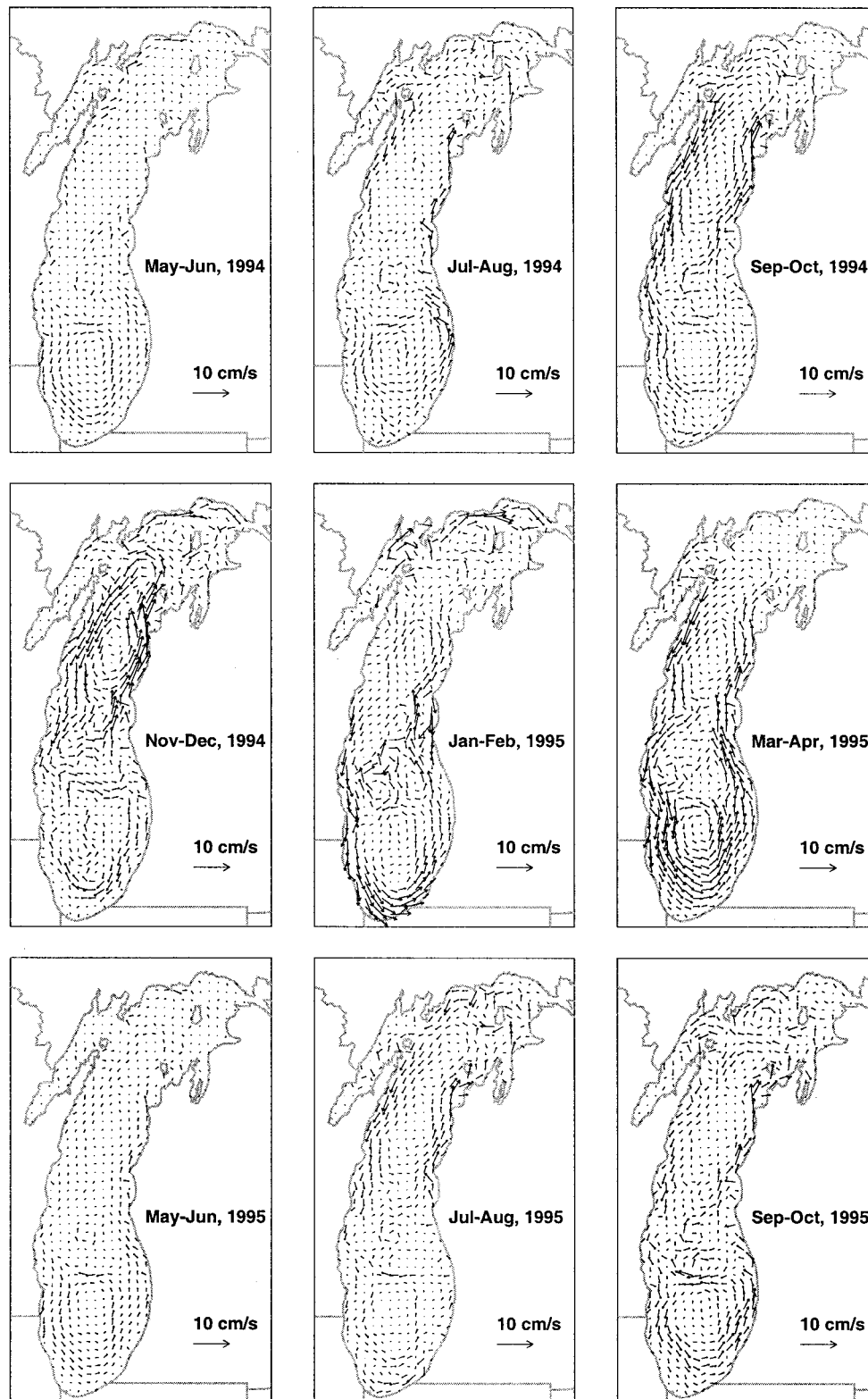
(b)

Figure 5.   (continued)

face temperature. In particular, the model predicted excessively high surface temperature in the Beaver Island area, which is especially evident during summer 1994 and 1995. In addition, in July–August 1994 and also in July–August 1995 the model produces stronger west coast upwelling, while in September-October and November-December 1994 the model underestimates this upwelling. These discrepancies can be mostly attributed to inaccuracies in the specification of forcing func-
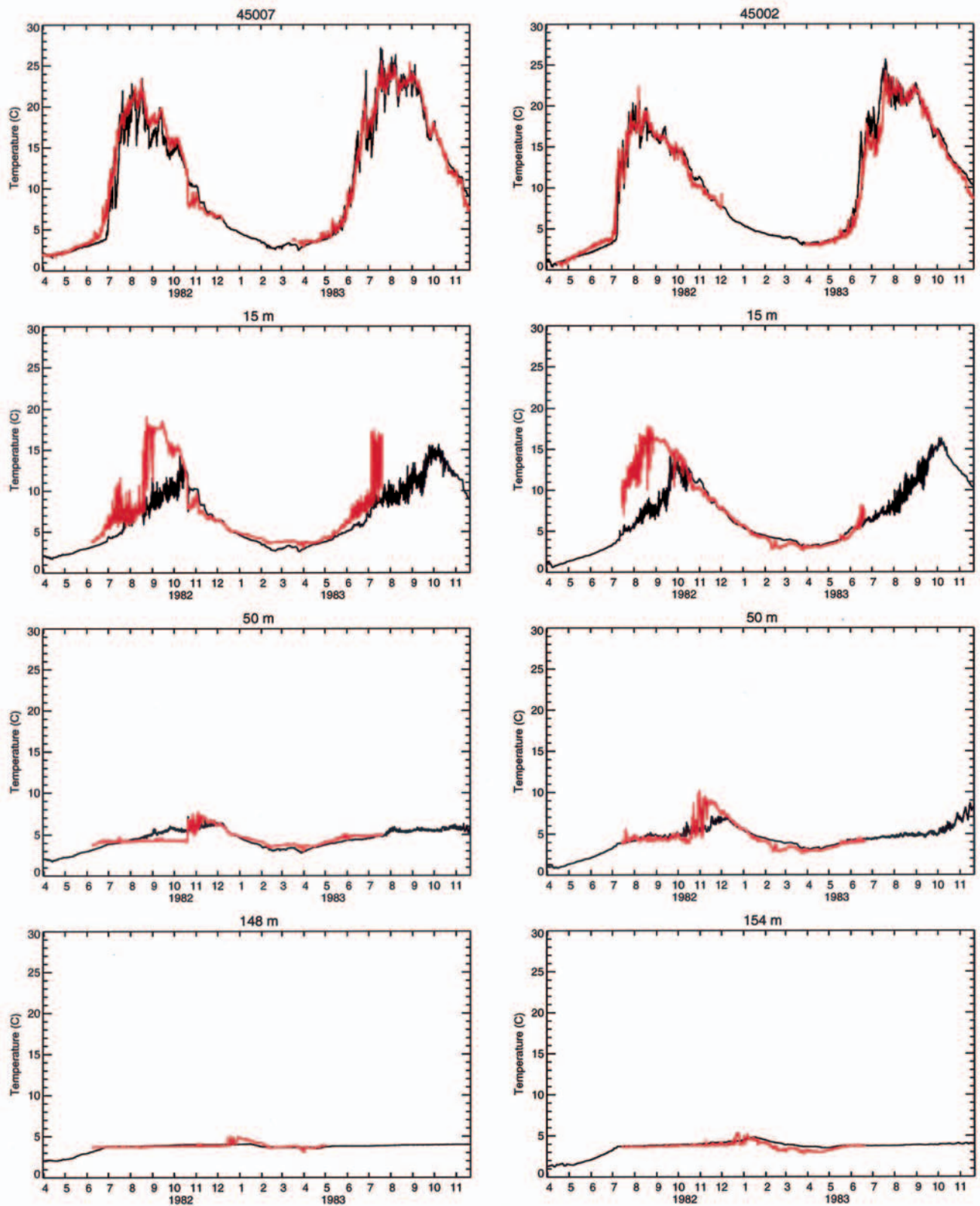
Plate 7. Time series of simulated (black line) water temperature versus observed (red line) at 45007 and 45002 in 1982–1983
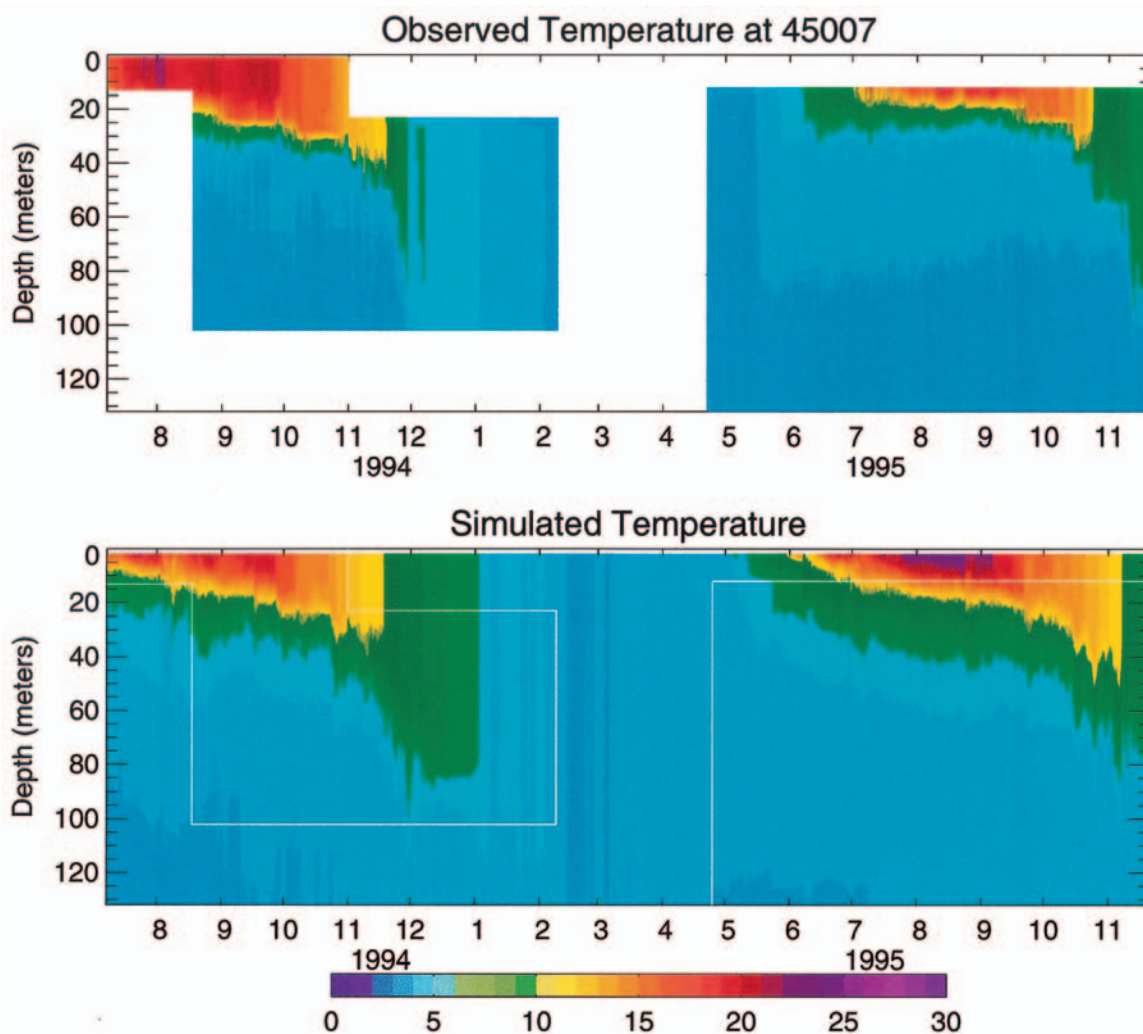
Plate 8.　Simulated and observed water temperature profile at buoy 45007 in 1994–1995.

tions such as wind speed (and direction), which affects coastal upwelling and both sensible and latent heat fluxes, and also cloud cover, which affects both short-wave and long-wave radiation. This hypothesis is supported by the fact that the largest errors are located in the Beaver Island area where the density of meteorological observations is smaller than that of the southern basin and other areas (Figure 1).

The fact of good agreement between the modeled surface temperature and remotely sensed temperature was corroborated by observations at three surface buoys in 1994–1995 (Plate 6). The accuracy of surface temperature predictions is similar in the first and second year of simulations, which we attribute to the rapid adjustment of the surface temperature field to the boundary conditions. In 1982–1983, in addition to surface temperature observations, there were also subsurface mooring data available at the 45002 and 45007 buoy locations (Plate 7). This data set shows that the comparison is quite good for the time evolution of the surface and bottom temperature, but it is worse in the thermocline area where modeled temperature is significantly lower than observed temperature during the first year. This may be a consequence of a too shallow or too diffuse model thermocline due to errors in initialization, vertical resolution, or model physics deficiencies. This was also true in 1994–1995 when another subsurface temperature data

set (although missing the upper layer in 1995) was available from a thermistor chain deployed near buoy 45007 located in the middle of the southern basin (Plate 8). The mixed layer in the model results is somewhat shallower than that in the observed temperature profile, a common feature of the Princeton model [*Martin*, 1985]. In addition, the modeled thermocline is too diffuse. In both 1982–1983 and 1994–1995, vertical temperature fluctuations due to internal waves in the modeled thermocline were not as pronounced as in observations.

Statistics of temperature time series comparisons at three surface buoy locations and 28 subsurface locations are presented in Table 1. There is high correlation between observed and modeled temperature. The root mean square difference is 0.7–2.5°C, and mean values are close.

5.3. Currents

For the purpose of model evaluation we compared bimonthly progressive vector diagrams of simulated and observed hourly currents at two depths (15 and 50 m). In general, currents exhibit vertical shear in summer and are more vertically uniform in winter (Plates 9a–9b). The largest currents occur in the fall, winter, and early spring, when temperature gradients are lowest but wind stresses are at their highest level. Nearshore currents appear to be much stronger than offshore

Plate 9. Progressive vector diagrams of simulated (black line) versus observed (red line) currents at (a) 15 and (b) 50 m in 1982–1983. The scale for progressive vector diagrams is also shown (made different from the lake scale to fit the figure).

currents, in agreement with existing conceptual models and observations [*Simons*, 1980; *Csanady*, 1982]. Still, even when driven by the nearshore currents similar to ones that are depicted in Plate 9, it takes a water parcel about a year to complete a round trip of Lake Michigan, which would be about 1000 km.

Point-to-point comparison of modeled and observed currents is a difficult task because of the strong spatial variability of lake currents especially in summer when the internal Rossby radius is close to the horizontal grid resolution. Thus, in July–August the 1982 observations at 15 m at mooring 1 do not exhibit the strong coastal current produced by the model. A strong anticyclonic gyre in the midlake plateau at both 15 and 50 m is barely seen in model results. In September–October, strong east coast currents in the model were also seen in

observations at 15 m at mooring 1, but modeled currents were opposite to observations at mooring 11, at mooring 23, and at mooring 5. Agreement was better at 50 m, indicating that this may be a result of an overly diffuse thermocline. During November–December 1982, modeled currents were in good agreement with observations although somewhat stronger at 15 m. During January–February 1983, agreement was good everywhere except at the midlake plateau. It was also true for March–April with the exception of model underprediction of currents at moorings 1 and 3. During May–June 1983, agreement was good except at the midlake plateau. Overall, the model performed better in terms of currents during January–April 1983 and worse during July–October 1982. Similar conclusions are supported by a more objective comparison of observed and modeled currents. The statistics of the compar-
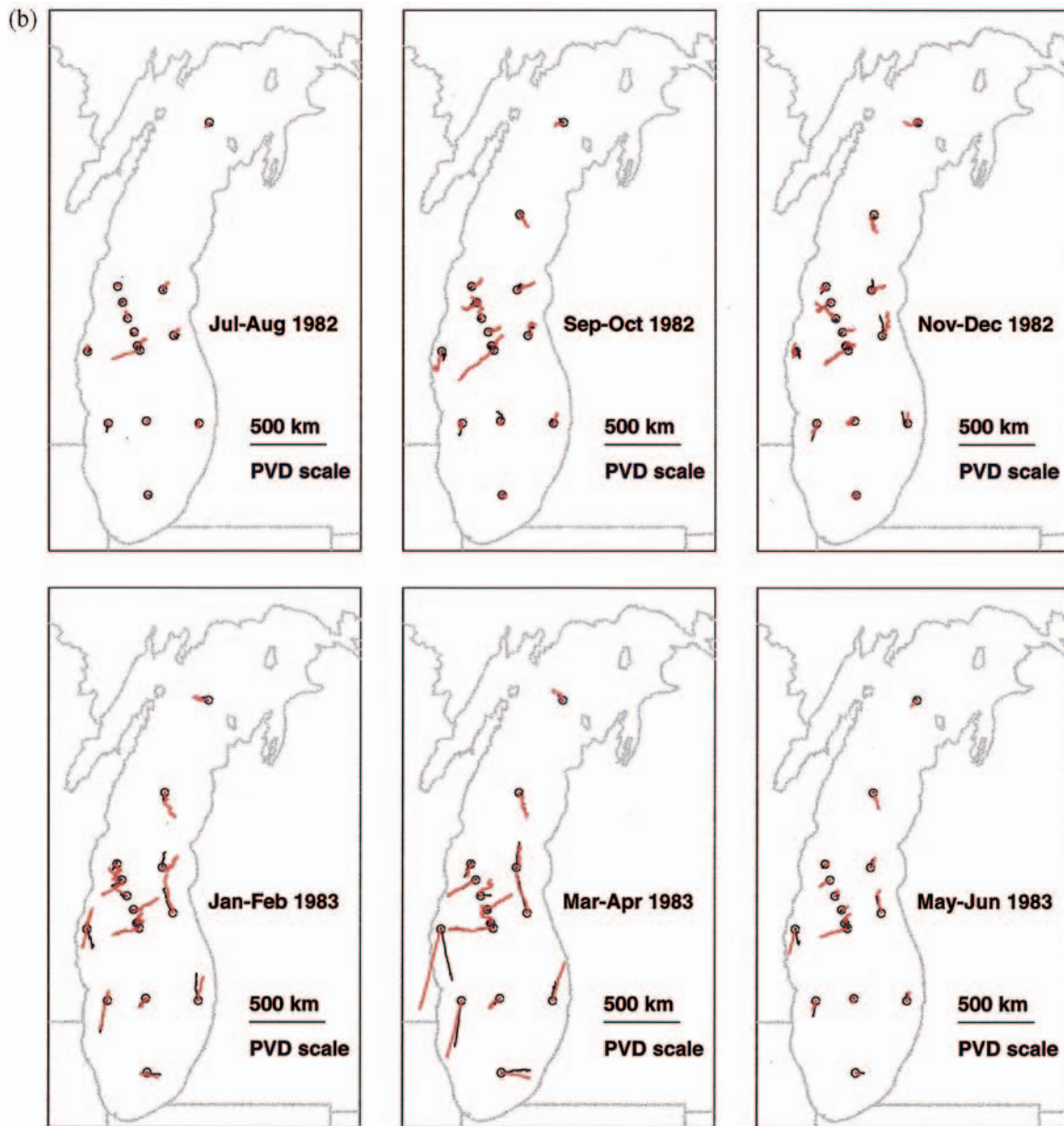
Plate 9. (continued)

ison between simulated and observed currents are presented in the form of the Fourier norms (rms difference). The Fourier norm of a time series of observed current vectors v_o and computed v_c is defined as

$$\|\mathbf{v}_o, \mathbf{v}_c\| = \left(\frac{1}{M} \sum_{t=\Delta}^{M\Delta t} |\mathbf{v}_o - \mathbf{v}_c|^2 \right)^{1/2}.$$

We use a normalized Fourier norm: $F_n = \|\mathbf{v}_o, \mathbf{v}_c\| / \|\mathbf{v}_o, 0\|$. The F_n can also be thought of as the relative percentage of variance in the observed currents that is unexplained by the calculated currents. In the case of perfect prediction, $F_n = 0$. In the case $0 < F_n < 1$, model predictions of current speed are better than no prediction at all (zero currents). Using F_n allows us to compare our model results more objectively with previous model results. For example, in one of the earlier modeling

exercises, *Allender* [1977] obtained $1.00 < F_n < 1.11$. Later, *Schwab's* [1983] results showed $0.79 < F_n < 1.01$. Both Allender and Schwab used a low-pass (48 hour) filter to eliminate near-inertial oscillations. We found in the 1982–1983 simulations $0.75 < F_n < 1.01$ for hourly currents. So, for the 1982–1983 simulations the hourly computed currents account for up to 25% of the total variance observed in the hourly current meter records. We also found that filtering out near-inertial oscillations with a period of 17 hours reduces F_n by about 10%. Figure 7 illustrates seasonal changes of F_n during July 1982 to June 1983. The model performed significantly better in winter with F_n around 0.70 for 15 m depth and 0.75 for 50 m depth. Nearshore currents (stations 1–4) were simulated even more accurately: F_n around 0.55 for 15 m depth and 0.60 for 50 m depth. On the contrary, summer currents were not predicted well: F_n was 0.95–1.05 for 15 m depth and 0.90–0.95 for 50 m depth.
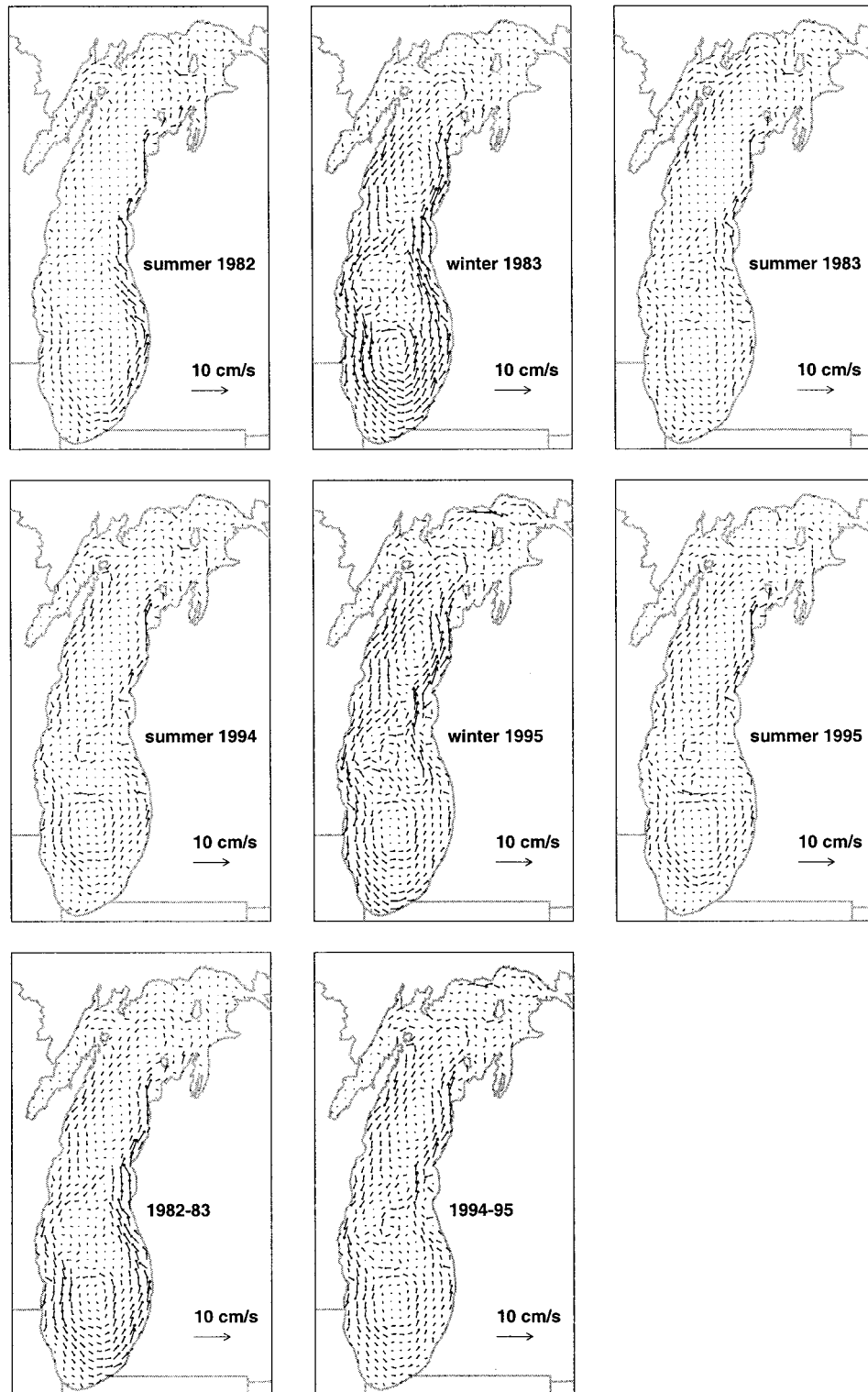
Figure 6. Six and 12 month averaged depth-averaged currents: 1982–1983 and 1994–1995.

Finally, we compared modeled currents with long-term averaged observations. Recent long-term current observations in Lake Michigan revealed a cyclonic large-scale circulation pattern, with cyclonic circulation within each subbasin and anticyclonic circulation in ridge areas [*Beletsky et al.*, 1999a] (Figure 8). Our model results coincide with these observations. Circulation is more organized and more cyclonic in winter than in summer, which is in agreement with earlier findings of *Saylor et al.* [1980]. Because winter circulation is stronger than summer circulation, annual circulation looks very similar to winter circulation. During summer 1982, lake-wide cyclonic circulation in the model (Figure 6) qualitatively matched observed circulation (Figure 8) and even stronger east coast than west coast currents were reproduced by the model. Observations

Table 1. Hydrodynamic Model Evaluations (Ensemble Averaged) for Surface Temperature at National Data Buoy Center Buoys (45002, 45007, and 45010) and Subsurface Temperature at Great Lakes Environmental Research Laboratory Current Meter Moorings (28 Instruments)

	Rms Difference	Mean Observed	Mean Modeled	Correlation Coefficient
Surface, 1994–1995	1.5	13.1	13.3	0.96
Surface, 1982–1983	1.2	12.1	12.1	0.99
15 m, 1982–1983	2.5	7.1	6.4	0.87
50 m, 1982–1983	0.7	4.2	4.3	0.78

revealed an anticyclonic gyre in the midlake plateau region with currents stronger than anywhere else in Lake Michigan at that time. This anticyclonic gyre was practically absent in modeled summer 1982 currents, too diffuse in winter 1982–1983, and clearly seen in summer 1983. Interestingly enough, this gyre was more pronounced in 1994–1995 modeled currents. During winter 1983 and the whole 1982–1983 period the model matched the general cyclonic circulation pattern, with cyclonic circulations in each subbasin and strong coastal currents.

6. Model Sensitivity Studies, Discussion, and Conclusions

This paper describes seasonal and annual circulation and temperature patterns in Lake Michigan obtained with a three-dimensional model and compares them to long-term observations. The results can be considered as a first step toward creating a climatology of circulation and temperature in Lake Michigan. Circulation was cyclonic during both stratified and nonstratified periods. An important question that needs to be addressed in future studies is whether cyclonic circulation in winter is typical or happens only during ice-free winters. The point is that winter meteorological conditions during the periods of study were climatologically unusual, while probably more typical for the mild winters of the 1990s. In addition, 1982–1983 and 1994–1995 can be considered to be "twin" periods: colder than normal winter followed by warmer than normal winter and warmer than normal summer. Moreover, surface wind patterns during these periods were also similar. Wind direction by itself probably does not matter in terms of the sign of mean currents. As our model results show, cyclonic circulation in Lake Michigan was generated by both northerly and southerly prevailing winds, but the presence of ice can also affect the vorticity of lake currents. Since mean annual circulation is mainly determined by winter circulation, this can also affect annual circulation patterns. Therefore there is clearly a need for a coupled ice-circulation model for long-term studies of lake hydrodynamics.

Overall, the model simulated the large-scale thermal structure and circulation quite realistically on the 5 km grid. Some previously observed characteristics of lake circulation [*Saylor et al.*, 1980] were reproduced by the model. In particular, the circulation was stronger in winter than in summer and also more organized and cyclonic, which is in agreement with observations. In summer, density-driven currents complicate lake hydrodynamics. Our LMMBS experience indicates that the contribution of density-driven currents is not as strong as that of wind-driven currents. For example, strong temperature (density) gradients were present in May–June 1982

(1994) versus weak gradients in May–June 1983 (1995), but total currents were almost the same. The strongest currents and maximum cyclonic vorticity were observed and modeled when the lake was either weakly stratified or homogeneous, from November until April. Since the lake is essentially homogeneous in winter, there are two probable explanations: existence of stronger cyclonic wind vorticity in winter or existence of residual mean cyclonic circulation driven by nonlinear interactions of topographic waves. D. J. Schwab and D. Beletsky (manuscript in preparation, 2001) address that issue more fully.

Finally, we want to address the problem of model accuracy, which depends on limitations of model physics, spatial discretization, and errors in specification of forcing functions and initial conditions. One of the limitations that we think may be due to model physics is that the model did not perform as well in the thermocline region as it performed near the surface. Internal waves were not as pronounced in the model as in observations. The simulated mixed layer was too shallow, as was previously shown by *Martin* [1985], and the thermocline was too diffuse. Temperature observations from several nearshore transects indicate that the problem of diffuse thermocline in the model is not limited to the offshore zone. We used very low background diffusivity in all model runs, 10^{-6} m^2 s^{-1}. Running the model with higher light extinction (optical category III) resulted in a slightly sharper thermocline but an even shallower mixed layer. To study the effect of vertical resolution on the vertical temperature gradients, we carried out a model run with 39 sigma levels, that is, double the vertical resolution. In this run we noticed only small improvement in the thermocline region. We also ran the model with zero horizontal diffusion to test for artificial diffusion along sigma surfaces [*Ezer and Mellor*, 2000]. Again, we did not notice a significant improvement in model results. Experiments with the improved version of the Mellor-Yamada model [*Mellor*, 2001] showed that it provides a deeper mixed layer, as was recently shown by *Ezer* [2000], but still too diffuse a thermocline. Clearly, more research is needed in order to understand what makes the model thermocline too diffuse.

The horizontal resolution of the model (5 km) was only sufficient for a description of large-scale circulation patterns (which happens to be of the most interest to LMMBS). The point-to-point comparison of mean currents was most successful in the southern basin, which is characterized by a relatively smooth bathymetry. It was more successful in fall-winter months than in summer (Plate 9), most probably because the horizontal resolution of the model is not adequate for proper simulation of baroclinic processes with horizontal length scales comparable to the Rossby deformation radius (which is around 5 km for summer months). In addition, model resolution was
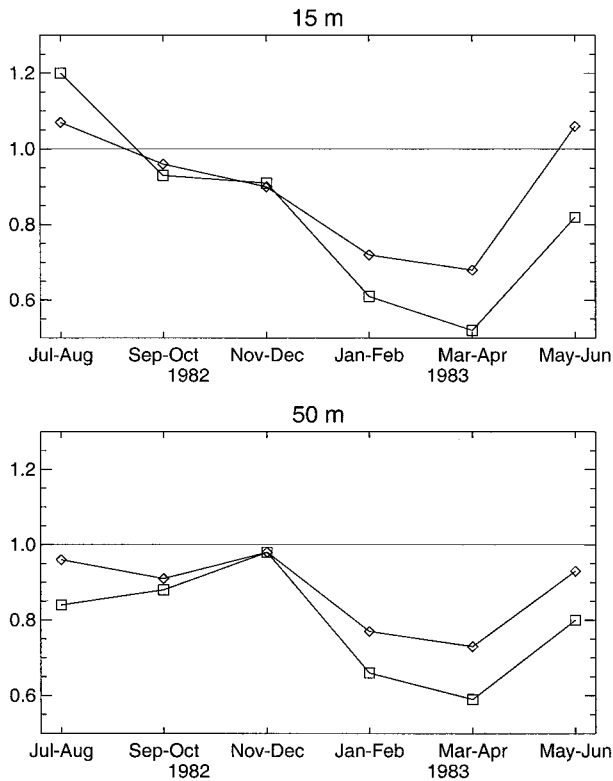
Figure 7. Ensemble-averaged Fourier norms calculated for six bimonthly periods during July 1982 to June 1983. Diamonds indicate all stations; squares indicate nearshore stations 1–4.

too coarse to describe precisely the hydrodynamics in the areas of strong depth gradients, even in the fall and winter when lake dynamics are essentially barotropic. Figure 7 shows that in areas of strong depth gradients the error does not decrease as significantly as in southern Lake Michigan (stations 1–4), which has rather smooth bathymetry and is well represented in the model. It is likely that finer grid resolution will significantly improve circulation model results in these areas in winter. The use of stretched grids may also be needed in order to improve circulation modeling in areas with steep depth gradients.

Finally, there is potential for improvement in the specification of forcing functions and initial conditions. Currently, meteorological observations are on the order of 30–50 km apart, which means that we may miss details of mesoscale meteorology. The network is less dense in the northern part of the lake, which can be the reason for larger errors in surface temperature compared with other parts of the lake. The 1994–1995 observation network had more stations than the 1982–1983 network, but model predictions did not improve noticeably. Perhaps the reason is that almost all new added stations were land stations, while the most significant changes in the mesoscale atmospheric characteristics should occur over water. Coupling meteorological and lake circulation models is the next logical step in improving atmospheric forcing used in the lake model. Initialization of the three-dimensional water temperature field also presents a significant challenge because only surface temperature from two National Data Buoy Center buoys is usually available for that purpose supplemented by episodic satellite observations.

Lake Michigan Averaged Currents, 1982-83
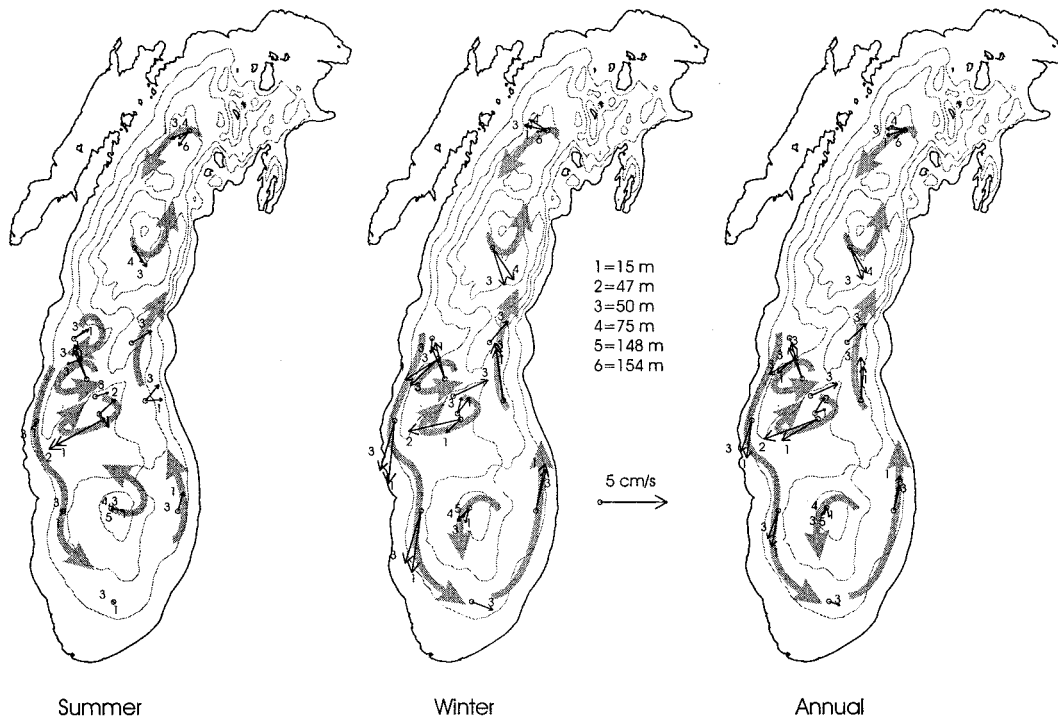
Figure 8. Observed mean circulation in Lake Michigan 1982–1983 from *Beletsky et al.* [1999a].

References

Allender, J. H., Comparison of model and observed currents in Lake Michigan, *J. Phys. Oceanogr.*, 7, 711–718, 1977.

Allender, J. H., and J. H. Saylor, Model and observed circulation throughout the annual temperature cycle of Lake Michigan, *J. Phys. Oceanogr.*, 9, 573–579, 1979.

Assel, R. A., F. H. Quinn, G. A. Leshkevich, and S. J. Bolsenga, *Great Lakes Ice Atlas*, Natl. Oceanic and Atmos. Admin. Great Lakes Environ. Res. Lab., Ann Arbor, Mich., 1983.

Assel, R. A., C. R. Snider, and R. Lawrence, Comparison of 1983 Great Lakes winter weather and ice conditions with previous years, *Mon. Weather Rev.*, 113, 291–303, 1985.

Assel, R. A., J. E. Janowiak, S. Young, and D. Boyce, Winter 1994 weather and ice conditions for the Laurentian Great Lakes, *Bull. Am. Meteorol. Soc.*, 77, 71–88, 1996.

Bedford, K. W., and D. J. Schwab, Preparation of real-time Great Lakes forecasts, *Cray Channels, Summer*, 14–17, 1990.

Beletsky, D., W. P. O'Connor, D. J. Schwab, and D. E. Dietrich. Numerical simulation of internal Kelvin waves and coastal upwelling fronts, *J. Phys. Oceanogr.*, 27, 1197–1215, 1997.

Beletsky, D., J. H. Saylor, and D. J. Schwab, Mean circulation in the Great Lakes. *J. Great Lakes Res.*, 25, 78–93, 1999a.

Beletsky, D., K. K. Lee, and D. J. Schwab, Large-scale circulation, in *Potential Climatic Effects on Lake Hydrodynamics and Water Quality* edited by D. Lam and W. M. Schertzer, pp. 4.1–4.41, Am Soc. of Civ. Eng., Reston, Va. 1999b.

Bennett, J. R., On the dynamics of wind-driven lake currents, *J. Phys. Oceanogr.*, 4, 400–414, 1974.

Bennett, J. R., A three-dimensional model of Lake Ontario's summer circulation, I, Comparison with observations, *J. Phys. Oceanogr.*, 7, 591–601, 1977.

Blumberg, A. F., Turbulent mixing processes in lakes, reservoirs and impoundments, in *Physics-Based Modeling of Lakes, Reservoirs, and Impoundments*, edited by W. G. Gray, pp. 79–104, Am. Soc. of Civ. Eng., New York, 1986.

Blumberg, A. F., and G. L. Mellor, A description of a three-dimensional coastal ocean circulation model, in *Three-Dimensional Coastal Ocean Models, Coastal Estuarine Sci.*, vol. 4, edited by N. S. Heaps, pp. 1–16, AGU, Washington, D. C., 1987.

Boyce, F. M., M. A. Donelan, P. F. Hamblin, C. R. Murthy, and T. J. Simons, Thermal structure and circulation in the Great Lakes, *Atmos. Ocean, 27*, 607–642, 1989.

Charnock, H., Wind stress on a water surface, *Q. J. R. Meteorol. Soc.*, 81, 639; 1955.

Csanady, G. T., *Circulation in the Coastal Ocean*, 279 pp. D. Reidel, Norwell, Mass. 1982.

Ezer, T., On the seasonal mixed layer simulated by a basin-scale ocean model and the Mellor-Yamada turbulence scheme, *J. Geophys. Res.*, 105, 16,843–16,855, 2000.

Ezer, T., and G. L. Mellor, Sensitivity studies with the North Atlantic sigma coordinate Princeton Ocean Model, *Dyn. Atmos. Oceans, 32*, 185–208, 2000.

Gottlieb, E. S., J. H. Saylor, and G. S. Miller, Currents and temperatures observed in Lake Michigan from June 1982 to July 1983, *NOAA Tech. Memo. ERL GLERL-71*, 45 pp., Natl. Oceanic and Atmos. Admin., Silver Spring, Md., 1989.

Jerlov, N. G., *Marine Optics*, 231 pp., Elsevier Sci., New York, 1976.

Kuan, C., K. W. Bedford, and D. J. Schwab, A preliminary credibility analysis of the Lake Erie portion of the Great Lakes Forecasting System for springtime heating conditions, in *Quantitative Skill Assessment for Coastal Ocean Models, Coastal Estuarine Stud.*, vol. 47, edited by D. R. Lynch and A. M. Davies, pp. 397–423, AGU, Washington, D. C., 1994.

Lam, D. C. L., and W. M. Schertzer (Eds.), *Potential Climatic Effects on Lake Hydrodynamics and Water Quality,* Am. Soc. of Civ. Eng., Reston, Va. 1999.

Liu, P. C., and D. J. Schwab, A comparison of methods for estimating u* from given uz and air-sea temperature differences, *J. Geophys. Res.*, 92, 6488–6494, 1987.

Long, P. E., and W. A. Shaffer, Some physical and numerical aspects of boundary layer modeling, *NOAA Tech. Memo. NWS TDL-56 (COM75-10980)*, Natl. Oceanic. and Atmos. Admin., Silver Spring, Md., 1975.

Lyons, W. A., Low level divergence and subsidence over the Great Lakes in summer, paper presented at 14th Conference on Great Lakes Research, Int. Assoc. for Great Lakes Res., Toronto, Ont., Can., 1971.

Martin, P. J., Simulation of the mixed layer at OWS November and Papa with several models, *J. Geophys. Res.*, 90, 903–916, 1985.

McCormick, M. J., and G. L. Fahnenstiel, Recent climatic trends in nearshore water temperatures in the St. Lawrence Great Lakes, *Limnol. Oceanogr.*, 44, 530–540, 1999.

McCormick, M. J., and D. C. L. Lam, Lake thermodynamics, in *Potential Climatic Effects on Lake Hydrodynamics and Water Quality*, edited by D. Lan and W. N. Schertzer, pp. 3.1–3.20, Am. Soc. of Civ. Eng., Reston, Va. 1999.

McCormick, M. J., and G. A. Meadows, An intercomparison of four mixed layer models in a shallow inland sea, *J. Geophys. Res., 93*, 6774–6788, 1988.

Mellor, G. L., An equation of state for numerical models of oceans and estuaries, *J. Atmos. Oceanic Technol.*, 8, 609–611, 1991.

Mellor, G. L., One dimensional, ocean surface layer modeling, a problem and a solution, *J. Phys. Oceanogr.*, 31, 790–809, 2001.

Mellor, G. L., and T. Yamada, Development of a turbulence closure model for geophysical fluid problems, *Rev. Geophys.*, 20, 851–875, 1982.

O'Connor, W. P., and D. J. Schwab, Sensitivity of Great Lakes Forecasting System nowcasts to meteorological fields and model parameters, paper presented at 3rd International Conference on Estuarine and Coastal Modeling, Am. Soc. of Civ. Eng. Waterw., Port, Coastal, and Ocean Div., Oak Brook, Ill., 1994.

Pettersen, S., and P. A. Calabrese, On some weather influences due to warming of the air by the Great Lakes in winter, *J. Meteorol.*, 16, 646–652, 1959.

Phillips, D. W., and J. G. Irbe, Lake to land comparison of wind, temperature, and humidity on Lake Ontario during the International Field Year for the Great Lakes (IFYGL), *Atmos. Environ. Serv. Rep. CLI-2-77*, Downsview, Ont., Can., 1978.

Rao, D. B., and T. S. Murty, Calculation of the steady-state wind-driven circulation in Lake Ontario, *Arch. Meteorol. Geophys. Bioklim., Ser. A, 19*, 195–210, 1970.

Resio, D. T., and C. L. Vincent, Estimation of winds over the Great Lakes, *J. Waterw. Port Coastal Ocean Div. 102*, 265–283, 1977.

Saylor, J. H., J. C. K. Huang, and R. O. Reid, Vortex modes in Lake Michigan, *J. Phys. Oceanogr.*, 10, 1814–1823, 1980.

Schertzer, W. M., and T. E. Croley, Climate and lake responses, in *Potential Climatic Effects on Lake Hydrodynamics and Water Quality*, edited by D. Lam and W. M. Schertzer, pp. 2.1–2.74, Am. Soc. of Civ. Eng., Reston, Va. 1999.

Schneider, K., R. A. Assel, and T. E. Croley II, Normal water temperature and ice cover of the Laurentian Great Lakes a computer animation, data base, and analysis tool, *NOAA Tech. Memo. ERL GLERL-81*, 47 pp., Natl. Oceanic and Atmos. Admin., Silver Spring, Md., 1993.

Schwab, D. J., Simulation and forecasting of Lake Erie storm surges, *Mon. Weather Rev. 106*, 1476–1487, 1978.

Schwab, D. J., Numerical simulation of low-frequency current fluctuations in Lake Michigan, *J. Phys. Oceanogr.*, 13, 2213–2224, 1983.

Schwab, D. J., A review of hydrodynamic modeling in the Great Lakes from 1950–1990 and prospects for the 1990's, in *Chemical Dynamics in Fresh Water Ecosystems*, edited by A. P. C. Gobas and A. McCorquodale, pp. 41–62, A. F. Lewis New York, 1992.

Schwab, D. J., and K. W. Bedford, Initial implementation of the Great Lakes Forecasting System: A real-time system for predicting lake circulation and thermal structure, *Water Pollut. Res. J. Can.*, 29, 203–220, 1994.

Schwab, D. J., and D. Beletsky, Lake Michigan Mass Balance Study— Hydrodynamic modeling project, *NOAA Tech. Memo. ERL GLERL-108*, 53 pp., Natl. Oceanic. and Atmos. Admin., Silver Spring, Md., 1998.

Schwab, D. J., and J. A. Morton, Estimation of overlake wind speed

from overland wind speed: A comparison of three methods, *J. Great Lakes Res*., *10*, 68–72, 1984.

Schwab, D. J., and D. L. Sellers, Computerized bathymetry and shorelines of the Great Lakes, *NOAA Data Rep. ERL GLERL-16*, 13 pp., Natl. Oceanic and Atmos. Admin., Silver Spring, Md., 1980.

Schwab, D. J., W. P. O'Connor, and G. L. Mellor, On the net cyclonic circulation in large stratified lakes, *J. Phys. Oceanogr*., *25*, 1516–1520, 1995.

Schwab, D. J., G. A. Leshkevich, and G. C. Muhr, Automated mapping of surface water temperature in the Great Lakes, *J. Great Lakes Res*., *25*, 468–481, 1999.

Semtner, A. J., Modeling ocean circulation, *Science, 269*, 1379–1385, 1995.

Simons, T. J., Verification of numerical models of Lake Ontario, I, Circulation in spring and early summer, *J. Phys. Oceanogr*., *4*, 507–523, 1974.

Simons, T. J., Verification of numerical models of Lake Ontario, II, Stratified circulations and temperature changes, *J. Phys. Oceanogr*., *5*, 98–110, 1975.

Simons, T. J., Verification of numerical models of Lake Ontario, III, Long-term heat transports, *J. Phys. Oceanogr*., *6*, 372–378, 1976.

Simons, T. J., Circulation models of lakes and inland seas, *Can. Bull. Fish. Aquat. Sci*., *203*, 146 pp., 1980.

Simons, T. J., Reliability of circulation models, *J. Phys. Oceanogr*., *15*, 1191–1204, 1985.

Thiessen, A. H., Precipitation average for large areas, *Mon. Weather Rev*., *39*, 1082–1084, 1911.

Wyrtki, K., The average annual heat balance of the North Pacific Ocean and its relation to ocean circulation, *J. Geophys. Res*., *70*, 4547–4599, 1965.

Xue, H., F. Chai, and N. R. Pettigrew, A model study of the seasonal circulation in the Gulf of Main, *J. Phys. Oceanogr*., *30*, 1111–1135, 2000.

Zavatarelli, M., and G. L. Mellor, A numerical study of the Mediterranean Sea circulation, *J. Phys. Oceanogr*., *25*, 1384–1414, 1995.

D. Beletsky and D. J. Schwab, NOAA Great Lakes Environmental Research Laboratory, 2205 Commonwealth Boulevard, Ann Arbor, MI 48105, USA. (beletsky@glerl.noaa.gov)